7-21-2022

# Evaluation of Nearshore Carbonate Chemistry Within Major Navigational Inlets of the Kristin Jacobs Coral Reef Ecosystem Conservation Area

Harrison Davis
*Nova Southeastern University*

# Thesis of
# Harrison Davis

Submitted in Partial Fulfillment of the Requirements for the Degree of

## Master of Science
## Marine Science

Nova Southeastern University
Halmos College of Arts and Sciences

July 2022

Approved:
Thesis Committee

Committee Chair: Tyler Cyronak

Committee Member: David Gilliam

Committee Member: Dorothy-Ellen A. Renegar

NOVA SOUTHEASTERN UNIVERSITY

HALMOS COLLEGE OF NATURAL SCIENCES AND OCEANOGRAPHY

# Evaluation of Nearshore Carbonate Chemistry Within Major Navigational Inlets of the Kristin Jacobs Coral Reef Ecosystem Conservation Area

By:

HARRISON DAVIS

Submitted to the Faculty of
Halmos College of Natural Sciences and Oceanography
in partial fulfillment of the requirements for
The degree of Master of Science with a specialty in:

Marine Science

Nova Southeastern University

August 2022

Thesis of

Harrison Davis

Submitted in Partial Fulfillment of the Requirements for the Degree of

Master of Science

Marine Science

Nova Southeastern University

Halmos College of Arts and Sciences

August 2022

Thesis Committee

Committee Chair: Tyler Cyronak, Ph.D

Committee Member: David Gilliam, Ph.D

Committee Member: Abigail Renegar, Ph.D

# Table of Contents

**ACKNOWLEDGEMENTS**

I would like to thank Dr. Tyler Cyronak for providing the materials, instruments, and consistent advisement over the course of this project. Thank you to Dr. David Gilliam for allowing this project to be completed in-parallel to the ongoing FDEP water quality assessment. Thank you, Dr. Abigail Renegar for providing advisement and support during the final phases of this project. I would like to extend thanks to the members of Dr. Tyler Cyronak and Dr. Dave Gilliam's labs for aiding in conceptual or statistical queries. I would like to thank The Florida Department of Environmental Protection Coral Protection and Restoration Program, especially Joanna Walczak, Jamie Monty, and Alycia Shatters, for funding the Kristin Jacobs Coral Ecosystem Conservation Area Water Quality Analysis Program. Finally, I would like to thank the members of the Nova FDEP water quality team for having the patience to allow me to complete my project while also working alongside them.

## LIST OF FIGURES

Figure 12. Demonstrates the significant linear relationship between the ratio of pH and Aragonite saturation state ($\Omega_{ARAG}$). Data points are black and the line of best fit (least squares method) is displayed in blue. The mean $\Omega_{ARAG}$ of these data is designated as a black horizontal dashed line, with the mean value displayed below the line.

Figure 13. Displays Latitude in relation to each inlet's TA-DIC slope, with a line of best fit (least squares) displayed in blue. Each data point represents an individual inlet location, with that inlet's TA-DIC slope value plotted on the X-axis and the latitude of the corresponding site plotted on the Y-axis. Each data point is accompanied by its respective name abbreviation to simplify identification. Inlets located closer to the Y-axis are more sensitive to DIC.

Figure 14. Demonstrates the sensitivity of individual inlets to DIC. The linear regressions defining each inlets relationship between TA and DIC or (TA-DIC) are displayed as dashed lines in greyscale. Inlet regressions are shaded lightest to darkest in increasing latitude, from south to north. Inlet GOC has the lightest shade of grey, while inlet STL has the darkest shade of grey. The regional TA-DIC trend is displayed as a solid black line. The approximate pH values of water samples at any given TA and DIC value are plotted in the background to demonstrate how each inlet's pH will change in response to DIC, with lower slope values crossing pH isoclines at more perpendicular angles.

## LIST OF TABLES

**ABSTRACT**

The absorption of atmospheric carbon dioxide ($CO_2$) by ocean surface water is causing ocean acidification (OA), a process by which the reaction between water and $CO_2$ changes ocean carbonate chemistry. Predictions of OA trajectories modeled by the Intergovernmental Panel on Climate Change (IPCC) are based on open ocean trends and may not accurately predict changes to variable nearshore ecosystems. The dynamic nature of nearshore ocean chemistry, and prevalence of OA vulnerable species within these ecosystems complicates the process of making accurate OA impact predictions within the coastal zone. Florida's coral reef is a nearshore ecosystem vulnerable to the effects of OA, as water chemistry along the east coast of Florida is influenced by the anthropogenically polluted and environmentally modified effluent carried out of its nearby inlets and waterways. Field samples collected during this study provide spatiotemporal data from 9 navigational inlets and five wastewater outfalls affecting the nearshore carbonate chemistry dynamics of the Kristin Jacobs Coral Ecosystem Conservation Area (Coral ECA) over the course of a year. Several notable trends were identified involving the carbonate system and associated environmental conditions. The concentrations of solutes in the freshwater endmembers were predicted through linear regressions with salinity and indicate that all inlets and outfalls within our sample region export greater amounts of inorganic carbon compared to alkalinity. The low ratio of alkalinity to dissolved inorganic carbon indicate that freshwater mixing could exacerbate ocean acidification in the nearshore coasts of South Florida. Furthermore, there was a trend between biogeochemical properties of the inlets with latitude, indicating diverse drivers of carbonate chemistry related to fundamental differences in the freshwater inputs along the coast. These results are intended to inform local and regional environmental management strategies with current and accurate carbonate chemistry measurements and may serve as environmental baselines by which future impact assessments may compare against.

Key Words: Ocean Acidification, Carbonate Chemistry, South Florida, Florida Reef Tract, Coral ECA, Kristin Jacobs Coral Ecosystem Conservation Area, Inlet, Total Alkalinity, Dissolved Inorganic Carbon, Outfall

## 1. INTRODUCTION

The decline in ocean surface water pH observed since the industrial era, known as ocean acidification (OA), is a consequence of the steadily increasing concentrations of atmospheric $CO_2$ (Doney et al., 2009). The pH of ocean surface water has already been reduced by 0.1 units, or roughly a 26% increase in acidity from preindustrial levels (IPCC, 2021). The Intergovernmental Panel on Climate Change (IPCC) has made several predictions for future changes in ocean pH across several $CO_2$ emissions scenarios and timescales, which have formed the basis for much of current OA research (IPCC, 2021). However, IPCC predictions are meant for the global open ocean and may not account for the natural variations in marine chemistry typical of nearshore ecosystems (Kapsenberg & Cyronak, 2019; Duarte et al., 2013). The limitation of these models in the coastal zone adds uncertainty to the results of studies focusing on organismal impacts of OA in nearshore environments (Rivest et al., 2017; Waldbusser & Salisbury, 2014; Price et al., 2012). Recognition of this disparity has motivated investigations into nearshore marine chemistry that attempt to define the spatial and temporal scales of variability to better inform OA impact assessments (Challener et al., 2015).

The effects of OA on marine organisms has been a primary research focus as of late, largely due to the negative impacts they are expected to experience (Kroeker et al., 2013). Capable of forming large calcium carbonate reef structures that support a tremendous amount of biodiversity, corals form the basis for diverse ecological communities when environmental conditions support their growth and accretion (Wilson et al., 2019; Fisher et al., 2015). Coral reefs provide numerous ecosystem services on local and global scales and have the potential to support local economies specializing in tourism and fisheries (Spalding et al., 2017). However, coral reefs are vulnerable to ocean acidification, particularly due to changes in calcification and dissolution of calcium carbonate ($CaCO_3$), which underpins the accretion of the structural components of a reef (Eyre et al., 2014; Chan & Connolly, 2013; Manzello et al., 2012). Given the range of chemistry changes expected to occur due to OA, a negative impact to coral survivability is expected. While the exact response of corals to acidification is species specific (Ries et al., 2009) it can be further complicated by other variables such as acclimation, local adaptation, and environmental variability (Cyronak et al., 2020; Rivest et al., 2017).

Coastal or nearshore marine environments already experience conditions similar or more extreme than those predicted by the IPCC (Krimsky et al., 2020; Rivest et al., 2017; Camp et al., 2016; Challener et al., 2015; Sunda & Cai, 2012). These variations are location specific, fluctuate over several timescales, and are influenced by the compounding effects of other anthropogenic disturbances (Pacella et al., 2018; Shaw et al., 2013). The instability of local environmental conditions is caused by multiple biotic and abiotic factors such as seasonal changes in solar irradiation, diel fluctuations in photosynthesis, respiration, and calcification, tidal mixing of water masses, environmental and metabolic sediment dissolution, and submarine groundwater discharge (Challener et al., 2015; Eyre et al., 2014; Duarte et al., 2013; Price et al., 2012). For example, nearshore environments such as seagrass beds, coral reefs, and mangroves can experience large diel fluctuations in pH (0.5-1 pH unit) and carbonate chemistry (Hunt, Salisbury, & Vandemark, 2022; Camp et al., 2016; Manzello et al., 2012). Across longer timescales, seasonal fluctuations in pH can be attributed to biotic and abiotic regime shifts in local biomass, temperature, or precipitation, typically ranging between 0.3 pH units or more in extreme cases (Duarte et al., 2013).

The southeast coastline of Florida offers a unique opportunity to study the dynamics of nearshore ocean chemistry. The shallow waters off the coast of Florida supports the third largest barrier reef in the world, known as the Florida Reef Tract (FRT). In total, the reef extends nearly 350 miles parallel to Florida's southeast coastline, beginning near the town of Port Saint Lucie and terminating in the Dry Tortugas. Scattered within and along the Florida reef are diverse mangrove and seagrass habitats, shallow bays, and waterways that contribute to this area's local carbonate chemistry regimes (Manzello et al., 2012). Not only do local habitats influence the local seawater chemistry, but each will be affected by OA in the coming century.

The northern most 105 miles of reef is known as the Kristin Jacobs Coral Reef Ecosystem Conservation Area (as of July 2021), formerly the Southeast Florida Coral Reef Ecosystem Conservation Area, or Coral ECA. This section of the Florida Reef Tract is under direct influence from Florida's Kissimmee, Okeechobee, and Everglades (KOE) watershed. Historically, the KOE watershed diverted water from central Florida's numerous lakes into the Okeechobee where it would then enter the Everglades. However, the development of agriculture and increased urbanization across southeast Florida necessitated the creation of canals and dikes

to manage flooding in urban environments and redirect water for agricultural use. The resulting network of shallow waterways have greatly altered the historic flow of water through Florida's natural KOE drainage basin, resulting in the divergence of approximately 70% of KOE water (Score & Jacoby, 2006). Water diverted from the KOE watershed towards the Atlantic Ocean flows through man-made canals and into Florida's Intracoastal Waterway (ICW). Effluent from the KOE watershed and engineered canals is introduced to the Atlantic Ocean through the ICW and any one of the nine ports or inlets along Florida's east coast (Figure 1). These ports and inlets are used for commercial and recreational boat traffic and navigation and are the only waterways through which terrestrial water is introduced to the Coral ECA, aside from municipal sewage outfalls and groundwater discharge. Agricultural wastes, floodwater, urban runoff, organic debris, and pollutants associated with anthropogenic disturbance flow through these inlets, potentially impacting coastal environmental health.

A previous investigation into the carbonate chemistry at three of the southern-most inlets along the Coral ECA demonstrated their potential to impact areas of the surrounding reef, acting as acidification hotspots (Enochs et al., 2019). Combined with evidence that reefs at the northernmost extent of the Coral ECA are already net erosional and experience seasonal $CaCO_3$ dissolution (Muehllehner et al., 2016), inlet water chemistry may play an important role in modulating reef biogeochemistry. These observations raise the question of whether water discharged from inlets or manmade effluent outfalls play a greater role in the fluctuations of carbonate chemistry at these northern inlet reefs compared to the more southerly reefs. Data suggests that the southern inlets are exporting disproportionately elevated DIC compared to TA to the surrounding reefs (Enochs et al., 2019). Discerning the influence that these ports and inlets have on the carbonate chemistry of its surrounding nearshore ecosystems is necessary for better understanding the current and future impacts of OA.

## 2. METHODS

### 2.1 Research Objective

The objective of this study was to characterize the temporal and spatial variability of carbonate chemistry within navigational inlets (n=9) and outfall surface boils (n=5) along the Coral ECA. Characterization of eight seawater chemistry parameters was conducted; temperature, salinity, total alkalinity (TA), dissolved inorganic carbon (DIC),

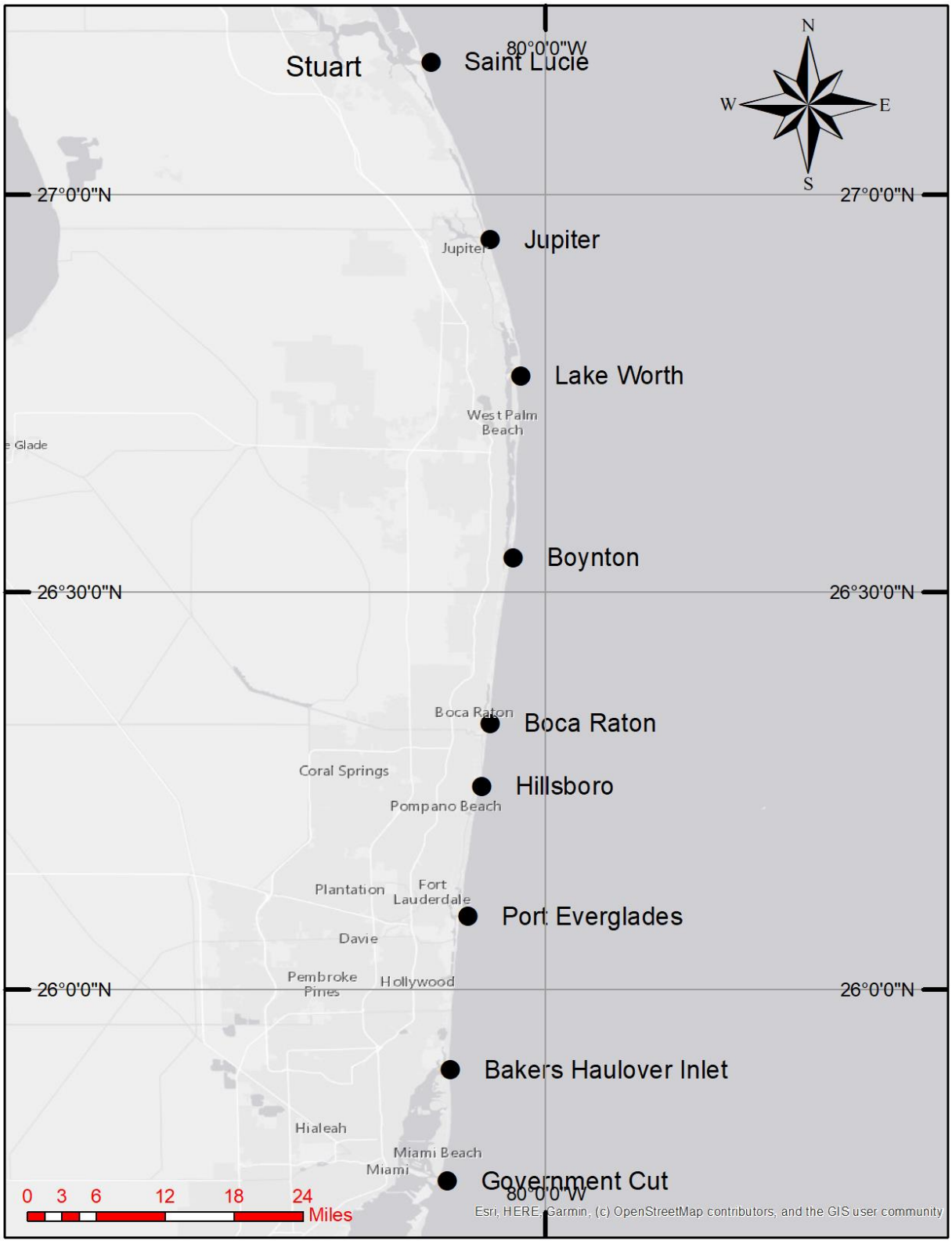


Figure 1. Regional study area with indicated inlet locations.

dissolved oxygen (DO), pH, aragonite saturation state ($\Omega_{ARAG}$), and the ratio of TA to DIC. Temporal variability of these eight parameters was assessed using data gathered during seven sampling periods (1-month duration each) and grouped into two distinct seasonal categories experienced within the study region: the wet (May-October) and dry (November-April) seasons. Spatial variability assessments were conducted by comparing inlet and outfall mean parameter values against the values of other inlet and outfall locations, as these locations are arranged across a latitudinal gradient with little longitudinal variation.

**2.2 Sampling Area**

This study features data collected from nine navigational inlets and five municipal wastewater outfalls (treated domestic sewage) located along the Coral ECA from Martin County to Miami-Dade County (Figure 1). This area comprises approximately 111 miles of Florida's coastline that has been divided into four individual counties, with a total population of about 6.3 million (U.S. Census Bureau, 2020). From north to south, the names and abbreviations of the inlets sampled during this investigation are as follows, with "*" given to those with wastewater outfalls located within their vicinity: Saint Lucie (STL), Jupiter (JUP), Lake Worth (ILW), Boynton Beach (BOY), Boca Raton* (BOC), Hillsboro* (HIL), Port Everglades* (PEV), Bakers Haulover* (BAK), and Government Cut* (GOC). An important feature of our study region is Florida's ICW that follows its coastline in parallel and functionally connects all nine inlets within our study area to both each other and the ocean.

Three of the nine inlets included within this study (GOC, PEV, and ILW) are ports used to accommodate large vessels including post-Panamax class container ships and cruise liners. These inlets have undergone extensive engineering and periodic maintenance to ensure their continued use, including modifications to their local habitats by dredging or removal of mangrove habitats for future expansion. The remaining six inlets are primarily used for domestic navigation of recreational vessels, typically maintained to shallower depths from 10-20 feet and experience less frequent periodic maintenance.

Wastewater outfall locations were included within this sampling regime to capture data on terrestrially influenced freshwater that is modifying this region's nearshore carbonate chemistry. Wastewater outfalls discharge terrestrially influenced freshwater that differs from inlet freshwater effluent in two main ways; (1) outfall wastewater effluent foregoes the biotic and

abiotic interactions that would have occurred during the effluent's entrainment within SE Florida's canals and ICW, and (2) outfall wastewater contains the treated sewage effluent from their respective municipalities and would be expected to influence carbonate chemistry parameters. This effluent is discharged offshore and at the sea floor, typically upwelling to the surface in an easily identifiable surface boil, which is where the sampling occurred.

**2.3 Experimental Design**

Inlet and outfall data collection began in July 2020 and was sampled on a bi-monthly basis between August 2020 and June 2021. In total, these data were collected across 7 sampling intervals over a period of 1 year. Each sampling interval was allocated to a single calendar month. During a designated sampling month, all 9 inlets were sampled, however the exact day and inlet sampled within that month was dependent on weather conditions. Data collected during the 7 sampling periods were grouped into two seasonal categories, the wet and dry seasons. Data collected during the months of November-April were grouped into the dry season, while data collected within the months of May-October were assigned to the wet season.

These data were collected at the water's surface only, with the sample site locations, geographic sampling positions, and collection timeframes used in this project in accordance with the methods specified by Whitall et al., 2020 (see pg 14-15). In summation of these methods, data collection occurred approximately two hours after high tide and before the proceeding low tide at four different geographic positions within each of the nine inlet sites. Inlet sampling positions are distributed as shown in Figure 2 at the north, south, east, and center of the inlet's ocean side effluent discharge. Sampling of wastewater outfalls was conducted at a single center position within the discharged surface boil. The data presented in this study are the product of 287 samples, with 28 cumulative samples per inlet and 7 total samples per outfall.

A handheld ProSolo YSI (Hydrolab) was used to collect and record measurements of dissolved oxygen (± 1%), salinity (± 1%), and temperature (± 0.2°C) at each water sampling location. Samples preserved for carbonate chemistry analysis (TA and DIC) were collected using best practices specified by Dickson et al., (2007). Temperature, salinity, and carbonate chemistry parameters were used to calculate the aragonite saturation state ($\Omega_{ARAG}$) and pH values for each sample using CO2SYS (Pierrot et al., 2006).

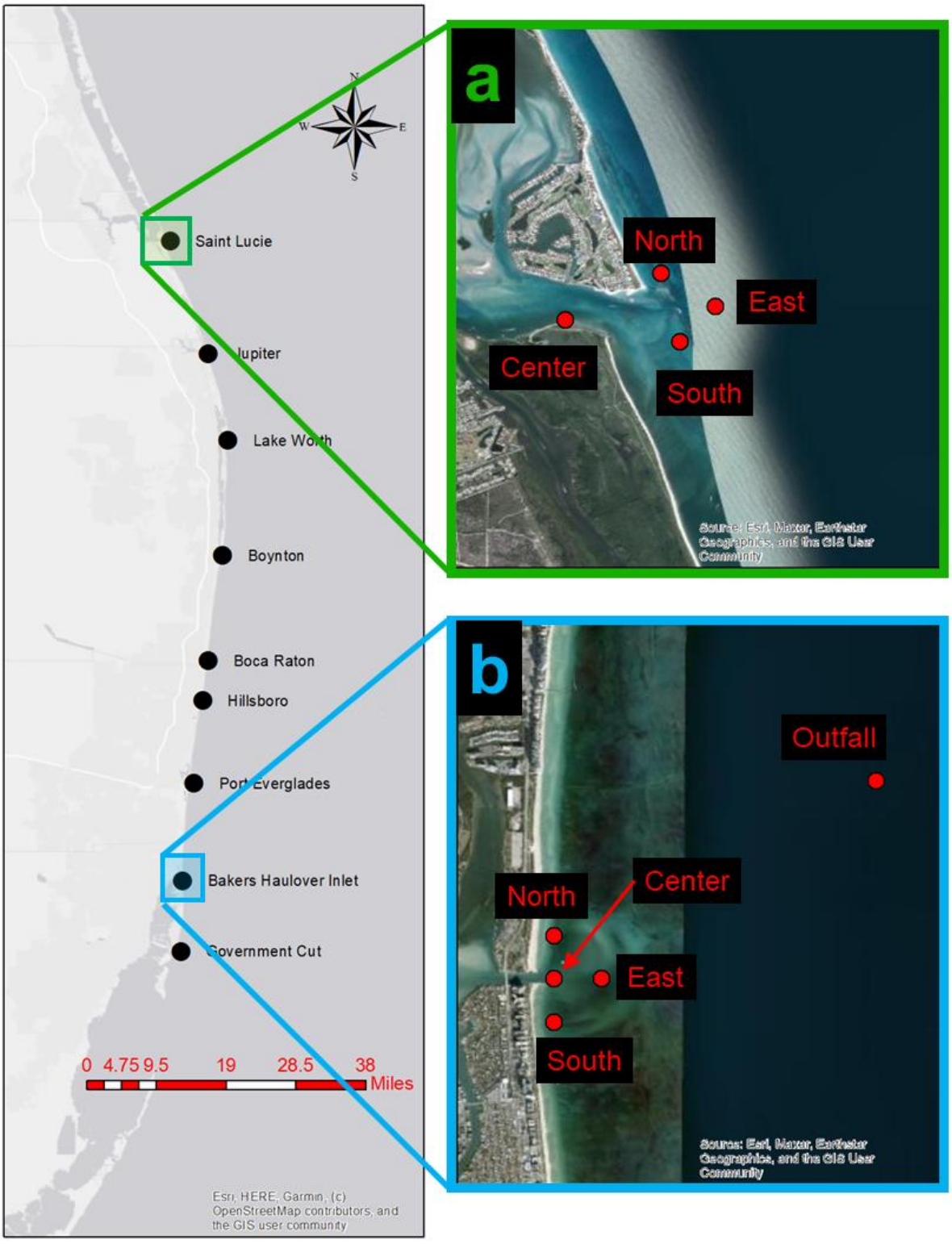


Figure 2. Map providing two examples of sample positions within inlet locations STL and BAK. (a) depicts Saint Lucie inlet (STL), demonstrating its abnormal center site arrangement and lack of an outfall site. (b) depicts Bakers Haulover inlet (BAK), demonstrating a typical inlet location site arrangement with an outfall location.

At each sampling location, a direct pull of surface water was collected from the stern of the vessel by fully submerging and retrieving a 12 L bucket. This served as the source water from which both the YSI measurements and discrete samples were taken. A 250 mL water sample was collected in a borosilicate glass vial, preserved with 100 µL of saturated $HgCl_2$, and sealed with Apiezon L grease. The samples were transported to the laboratory and stored at room temperature (approx. 20°C) until total alkalinity and dissolved inorganic carbon analyses could be completed.

Laboratory analysis of total alkalinity was conducted by open-cell potentiometric acid titration. The instrument used for this measurement was an 888 Metrohm Titrando titrator with an 806 Dosimat and Metrohm pH electrode. Dissolved inorganic carbon measurements were determined using a custom-built system with Li-COR 850 $CO_2$ analyzer following the procedures detailed by Dickson et al., (2007; see SOP 2 and 3B). Certified reference materials (CRM batch 184; (Dickson et al., 2007)) were used to validate the accuracy and precision of these laboratory instruments (TA= 2226.44 ± 2.0, DIC= 2099.1 ± 9.7; mean ± SD).

The ProSolo YSI digital water quality meter was calibrated using its onboard calibration feature with 47600 µS/cm (0.51 Normal) standard calibration solution (RICCA Chemical Company). Oxygen was calibrated to 100% saturated air. Calibrations for salinity and dissolved oxygen were conducted before each sampling month and checked throughout that month's sampling period.

Data interpretation and statistical analysis was conducted using the statistical computing software R (R Core Team, 2021). Spatial variability assessments of inlet data were based on inlet-to-inlet comparisons using rank-sum transformed one-way repeated measures ANOVAs. Temporal variability assessments conducted between season (wet/dry) and site type (inlet/outfall) were based on Kruskal-Wallis chi-squared tests. Linear regression models were used to define parameter-parameter relationships and any significant relationships reported were based on each relationship's corresponding F-statistic using a confidence interval of at least 95%. ArcMap, an application within the ArcGIS software suite, was used to create various Figures that describe the sample locations and geographic sampling positions at each inlet and outfall.

## 3. RESULTS

### 3.1 Inlet Water Chemistry

Overall, inlet location had a significant effect on temperature, salinity, DO, pH, and $\Omega_{ARAG}$ (p-value < 0.05). While sample location (inlet name/identity) did not significantly affect TA or DIC, significant differences in the TA/DIC ratio were detected. While significant differences were detected in environmental parameters between the different inlets, the magnitude of differences between the means were relatively small compared to the large variability at any given site (Table 1, Figure 3). The highest mean temperatures and salinities were both observed at inlet BAK, while the lowest mean temperatures and salinities were observed at inlet STL. On average, DO concentrations were greatest at inlet HIL and lowest at inlet PEV. Lake Worth inlet experienced the highest average pH, while PEV experienced the lowest mean pH. Government cut inlet had the highest mean $\Omega_{ARAG}$ while inlet STL saw the lowest mean $\Omega_{ARAG}$.

Season was found to have a significant effect on temperature, DO, and pH. The effect of season was less nuanced than inlet location, characterized by a warm wet season whose temperatures were several degrees higher on average (29.2 ± 1.3°C; mean ± SD) than the cooler dry season (23.9 ± 1.6°C). The wet season was also accompanied by lower mean DO (188 ± 10.5 µmol $kg^{-1}$) and pH (7.83 ± 0.08) values than in the dry season. The elevated levels of DO (213 ± 7.0 µmol $kg^{-1}$) and pH (7.95 ± 0.04) during the dry season were likely caused by reduced seawater temperatures.

While the effects of season on salinity, TA, DIC, $\Omega_{ARAG}$, and TA/DIC ratios were not significant, season generally imparted greater variability in these environmental parameters during the wet season than the dry (Figures 4 and 5). Across inlets, mean salinity values during the wet season (34.5 ± 3.6) were fairly similar to those observed during the dry (34.6 ± 1.7) season. The wet season experienced salinity variances over a range of 26.0 PSU as opposed to the dry season's range of 12.5 PSU. Mean TA and DIC values were relatively similar across seasons, with slightly lower mean DIC values (2157.5 ± 46 µmol $kg^{-1}$) in the dry season. Total alkalinity ranged between 2177-2752 µmol $kg^{-1}$ during the wet season and 2334-2552 µmol $kg^{-1}$ during the dry. Seasonal ranges of DIC were more extreme during the wet season than the dry,

Table 1. Values are mean environmental conditions with (Standard Deviation) across Wet and Dry seasons.

| | Temperature (°C) | | Salinity (PSU) | | Dissolved Oxygen ( µmol $kg^{-1}$) | | Total Alkalinity ( µmol $kg^{-1}$) | | Dissolved Inorganic Carbon( µmol $kg^{-1}$) | | TA/DIC Ratio | | pH | | ΩArag | |
|---|---|---|---|---|---|---|---|---|---|---|---|---|---|---|---|---|
| | Wet | Dry | Wet | Dry | Wet | Dry | Wet | Dry | Wet | Dry | Wet | Dry | Wet | Dry | Wet | Dry |
| **Government Cut (GOC)** | | | | | | | | | | | | | | | | |
| Inlet | 29.9 (1.4) | 24.1 (2.0) | 35.7 (1.9) | 34.2 (1.5) | 188 (5) | 212 (4) | 2354 (77) | 2436 (58) | 2114 (93) | 2185 (76) | 1.11 (0.015) | 1.12 (0.013) | 7.85 (0.04) | 7.96 (0.05) | 2.88 (0.19) | 2.97 (0.17) |
| Outfall | 28.8 (1.4) | 24.8 (0.35) | 36.0 (1.5) | 34.9 (1.3) | 189 (6) | 205 (4) | 2406 (13) | 2410 (12) | 2189 (35) | 2194 (46) | 1.10 (0.013) | 1.10 (0.017) | 7.81 (0.04) | 7.88 (0.05) | 2.65 (0.21) | 2.60 (0.30) |
| **Bakers Haulover (BAK)** | | | | | | | | | | | | | | | | |
| Inlet | 30.2 (1.1) | 25.6 (0.84) | 36.1 (1.2) | 34.9 (0.68) | 186 (9) | 210 (5) | 2395 (58) | 2409 (20) | 2153 (71) | 2164 (26) | 1.11 (0.013) | 1.11 (0.0077) | 7.84 (0.04) | 7.92 (0.03) | 2.91 (0.21) | 2.91 (0.13) |
| Outfall | 29.1 (1.5) | 25.0 (0.00) | 36.9 (1.5) | 34.9 (1.0) | 193 (7) | 212 (4) | 2393 (15) | 2410 (6) | 2139 (42) | 2173 (7) | 1.12 (0.015) | 1.11 (0.0040) | 7.87 (0.05) | 7.92 (0.004) | 2.99 (0.24) | 2.81 (0.052) |
| **Port Everglades (PEV)** | | | | | | | | | | | | | | | | |
| Inlet | 29.7 (0.72) | 23.3 (1.8) | 35.7 (1.5) | 34.8 (0.26) | 182 (8) | 213 (4) | 2428 (57) | 2412 (38) | 2196 (76) | 2169 (45) | 1.11 (0.012) | 1.11 (0.0078) | 7.83 (0.04) | 7.96 (0.04) | 2.84 (0.15) | 2.82 (0.094) |
| Outfall | 28.9 (1.0) | 24.3 (1.7) | 36.4 (1.1) | 34.1 (0.95) | 193 (9) | 201 (8) | 2383 (10) | 2408 (14) | 2152 (79) | 2303 (54) | 1.11 (0.036) | 1.05 (0.018) | 7.83 (0.1) | 7.64 (0.1) | 2.78 (0.69) | 1.58 (0.31) |
| **Hillsboro (HIL)** | | | | | | | | | | | | | | | | |
| Inlet | 29.4 (1.4) | 23.7 (1.4) | 34.4 (2.4) | 34.5 (1.8) | 193 (14) | 213 (10) | 2425 (57) | 2401 (28) | 2203 (81) | 2154 (56) | 1.10 (0.018) | 1.12 (0.015) | 7.83 (0.06) | 7.96 (0.04) | 2.77 (0.30) | 2.89 (0.23) |
| Outfall | 28.9 (1.4) | 24.1 (1.0) | 36.3 (1.4) | 34.6 (1.2) | 190 (12) | 204 (5) | 2400 (22) | 2402 (1) | 2142 (45) | 2160 (17) | 1.12 (0.013) | 1.11 (0.0089) | 7.88 (0.05) | 7.94 (0.03) | 3.05 (0.20) | 2.85 (0.14) |
| **Boca Raton (BOC)** | | | | | | | | | | | | | | | | |
| Inlet | 28.9 (1.4) | 24.7 (1.6) | 32.6 (6.3) | 35.3 (0.82) | 189 (9) | 209 (10) | 2443 (98) | 2396 (22) | 2250 (179) | 2144 (37) | 1.09 (0.038) | 1.12 (0.010) | 7.79 (0.1) | 7.95 (0.03) | 2.52 (0.63) | 2.94 (0.16) |
| Outfall | 28.7 (1.1) | 24.8 (1.3) | 36.2 (1.4) | 35.5 (0.61) | 192 (8) | 208 (12) | 2429 (67) | 2414 (35) | 2174 (86) | 2152 (37) | 1.12 (0.016) | 1.12 (0.0032) | 7.88 (0.05) | 7.96 (0.03) | 3.03 (0.21) | 3.05 (0.017) |
| **Boynton (BOY)** | | | | | | | | | | | | | | | | |
| Inlet | 28.8 (0.71) | 23.6 (0.77) | 33.5 (3.3) | 34.9 (1.4) | 190 (11) | 215 (6) | 2396 (38) | 2409 (38) | 2190 (61) | 2157 (55) | 1.09 (0.027) | 1.12 (0.012) | 7.82 (0.08) | 7.97 (0.02) | 2.60 (0.48) | 2.93 (0.17) |
| **Lake Worth (ILW)** | | | | | | | | | | | | | | | | |
| Inlet | 28.6 (1.4) | 23.5 (0.88) | 34.1 (5.7) | 35.2 (0.70) | 194 (7) | 211 (6) | 2411 (50) | 2391 (16) | 2177 (104) | 2137 (38) | 1.11 (0.029) | 1.12 (0.013) | 7.86 (0.06) | 7.97 (0.04) | 2.85 (0.48) | 2.94 (0.25) |
| **Jupiter (JUP)** | | | | | | | | | | | | | | | | |
| Inlet | 28.7 (1.4) | 23.9 (0.49) | 34.7 (2.6) | 34.9 (0.35) | 183 (12) | 213 (2) | 2384 (35) | 2389 (20) | 2165 (36) | 2138 (25) | 1.10 (0.026) | 1.12 (0.0069) | 7.83 (0.1) | 7.96 (0.03) | 2.69 (0.48) | 2.92 (0.13) |
| **Saint Lucie (STL)** | | | | | | | | | | | | | | | | |
| Inlet | 28.5 (1.1) | 22.6 (1.8) | 34.0 (2.9) | 32.8 (3.7) | 188 (12) | 218 (8) | 2373 (65) | 2388 (32) | 2157 (46) | 2170 (31) | 1.10 (0.024) | 1.10 (0.019) | 7.84 (0.09) | 7.94 (0.04) | 2.67 (0.45) | 2.60 (0.35) |

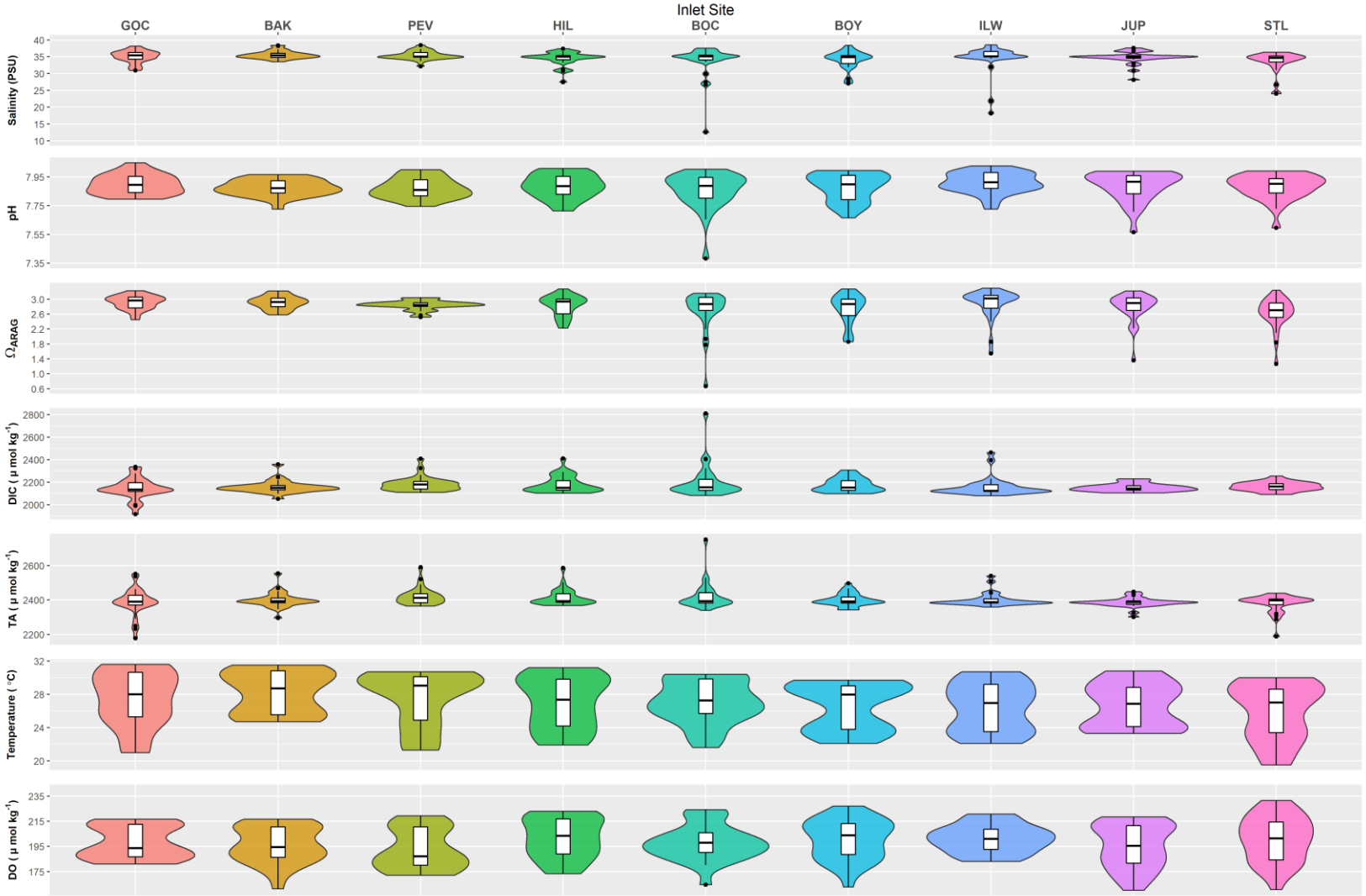


Figure 3. Violin plots for each water quality parameter across all 9 inlets. Y-axis labels indicate the measured parameter and the X-axis displays the abbreviated name for each inlet. Inlets are color coded, listed on the X-axis left to right in increasing latitude, from south to north.

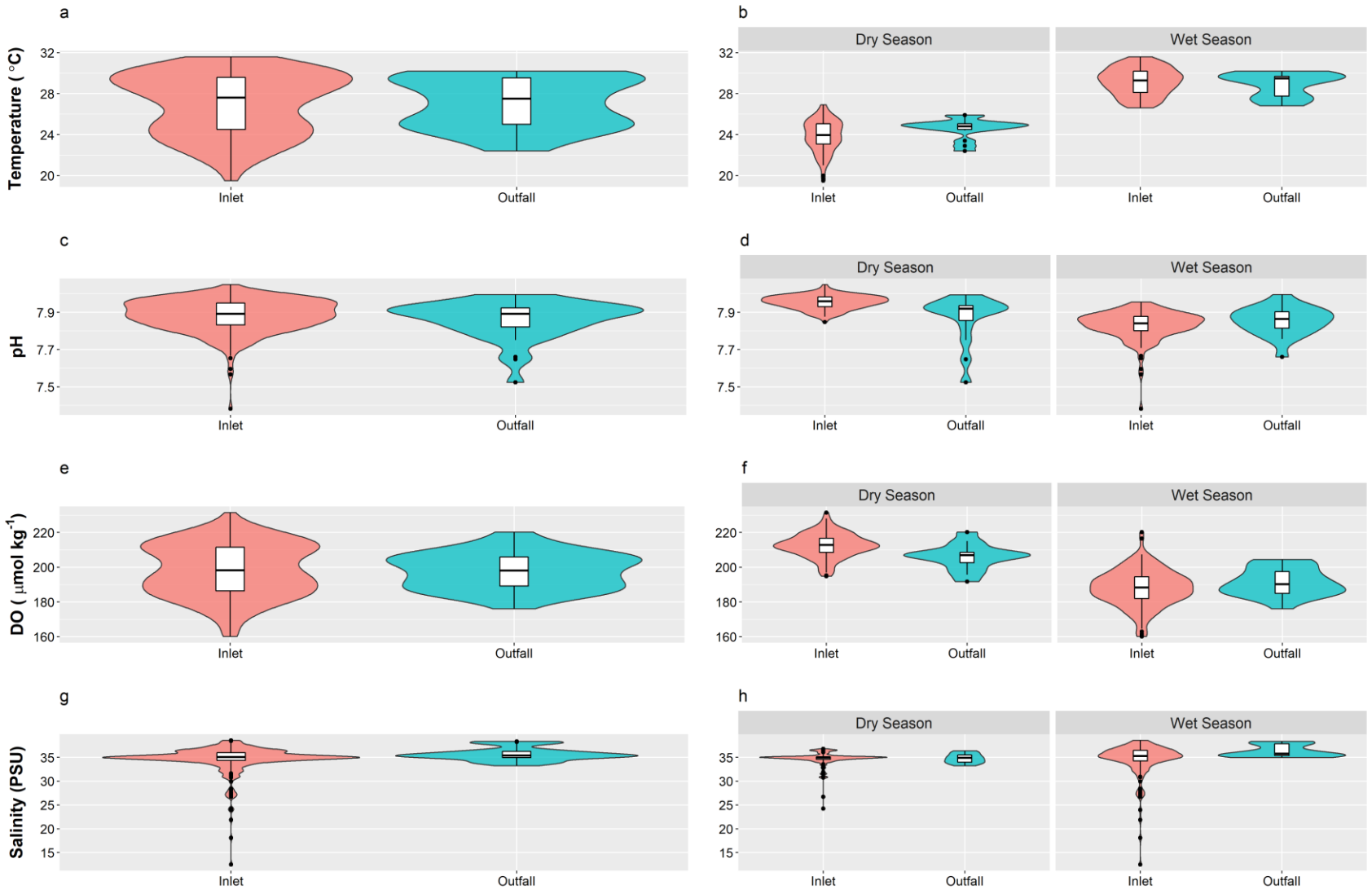


Figure 4. From top to bottom, violin plots of temperature, pH, dissolved oxygen, and salinity both across (a,c,e, g) and within (b,d,f, h) the wet (right) and dry (left) seasons. Site types have been color coded, pink for inlet data and blue for outfall data.

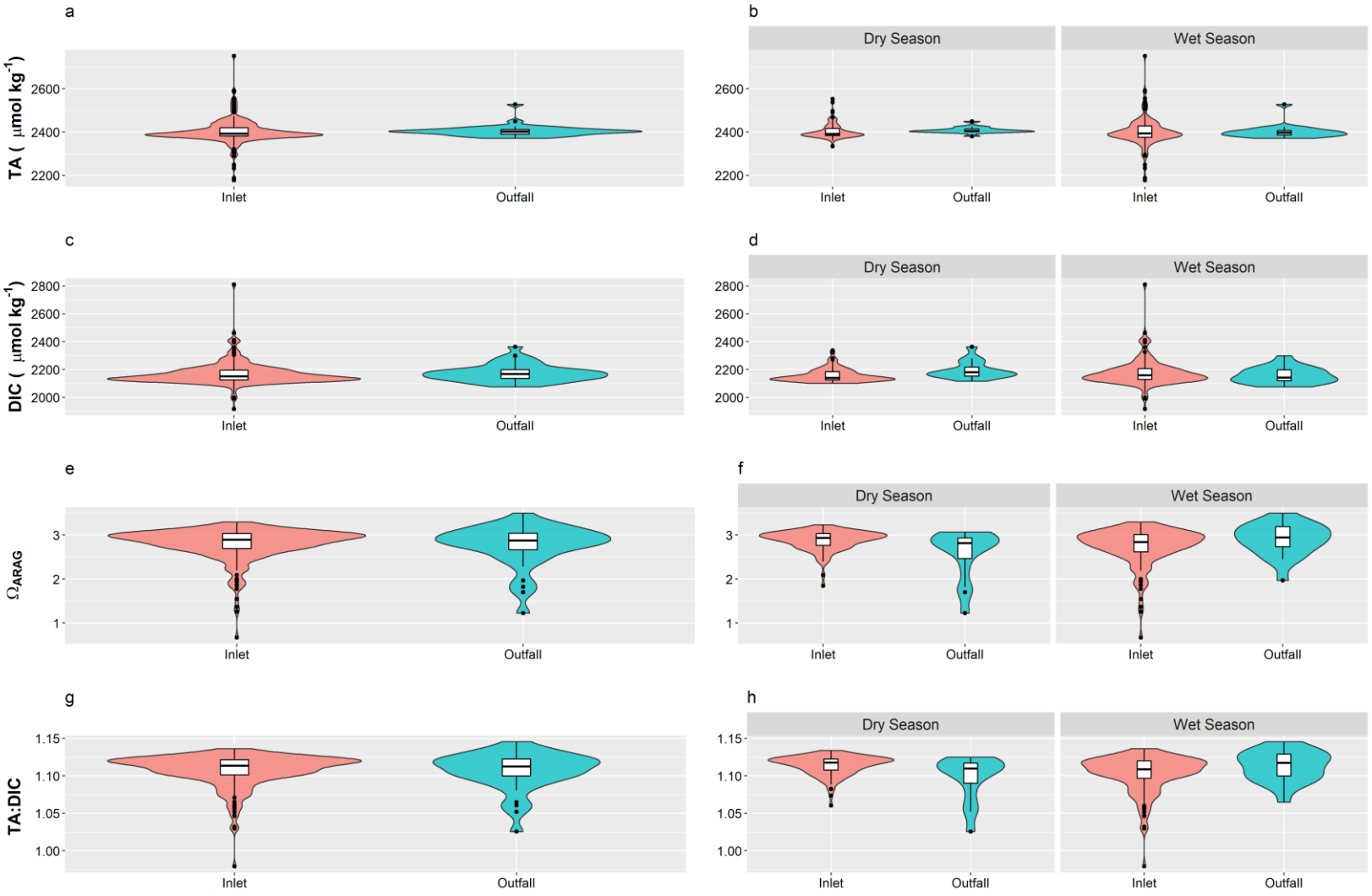


Figure 5. From top to bottom, violin plots of total alkalinity, dissolved inorganic carbon, aragonite saturation state ($\Omega_{ARAG}$), and TA:DIC both across (a,c,e, g) and within (b,d,f, h) the wet (right) and dry (left) seasons. Site types have been color coded, pink for inlet data and blue for outfall data.

occurring over 1917-2810 µmol $kg^{-1}$ and 2100-2337 µmol $kg^{-1}$ for the wet and dry seasons respectively. Aragonite saturation states were lower in the wet (3 ± 0.4) season than the dry (3 ±0.2) season. The ratio of TA to DIC was nearly identical across seasons, with (1.1 ± 0.02) and (1.1 ± 0.01) for the wet and dry seasons respectively.

### 3.2 Regression Analysis

Across season and sample location, salinity was found to have significant relationships with temperature, DIC, TA, pH, $\Omega_{ARAG}$, and TA/DIC ratios. When all the data was grouped together, both TA and DIC (Figure 6) were significantly negatively correlated with salinity. However, the slope of the linear regression between DIC and salinity was more negative (-19.2 µmol $kg^{-1}$ $S^{-1}$) than the slope of the linear regression between TA and salinity (-7.1 µmol $kg^{-1}$ $S^{-1}$). The fit of these relationships was low for TA ($R^2$= 0.15, $p < 0.001$) but moderate for DIC ($R^2$=0.51, $p < 0.001$), with zero salinity endmembers (e.g. y-intercepts) of 2646 µmol $kg^{-1}$ for TA and 2831 µmol $kg^{-1}$ for DIC. These regional and inlet specific TA, DIC, and TA:DIC zero salinity endmembers are summarized in Table 2.

While a general relationship between TA versus salinity and DIC versus salinity was identified when all the data was grouped together, differences were detected between inlets. All inlets besides BOY and BAK demonstrated significant positive and negative relationships with TA and salinity (Figure 7). Within these significant relationships, $R^2$ values ranged from 0.22 at inlet JUP to 0.90 at inlet BOC, indicating a variable impact of salinity as a descriptor of TA values. Total alkalinity endmembers predicted by these significant relationships ranged from 2015 µmol $kg^{-1}$ at inlet STL to 3273 µmol $kg^{-1}$ at inlet GOC. Similarly, all inlets besides BAK and STL demonstrated a significant relationship between DIC and salinity. The $R^2$ values for inlets with significant relationships between DIC and salinity ranged from 0.28-0.92 at inlet sites PEV and BOC respectively, indicating a similar range of descriptive power of salinity for DIC. Predicted endmembers from these significant relationships ranged from 2549 µmol $kg^{-1}$ DIC at inlet JUP to 3287 µmol $kg^{-1}$ DIC at inlet GOC. All inlets demonstrated significant positive relationships between the ratio of TA to DIC and salinity (Figure 8 and 9). The ratio of TA to DIC versus salinity demonstrated an adjusted $R^2$ value of 0.69 for all data, however the adjusted $R^2$ values for the individual TA:DIC relationships ranged from 0.16 at site BAK to 0.85 at site BOC. Inlet specific TA and DIC endmembers had a significant negative relationship with

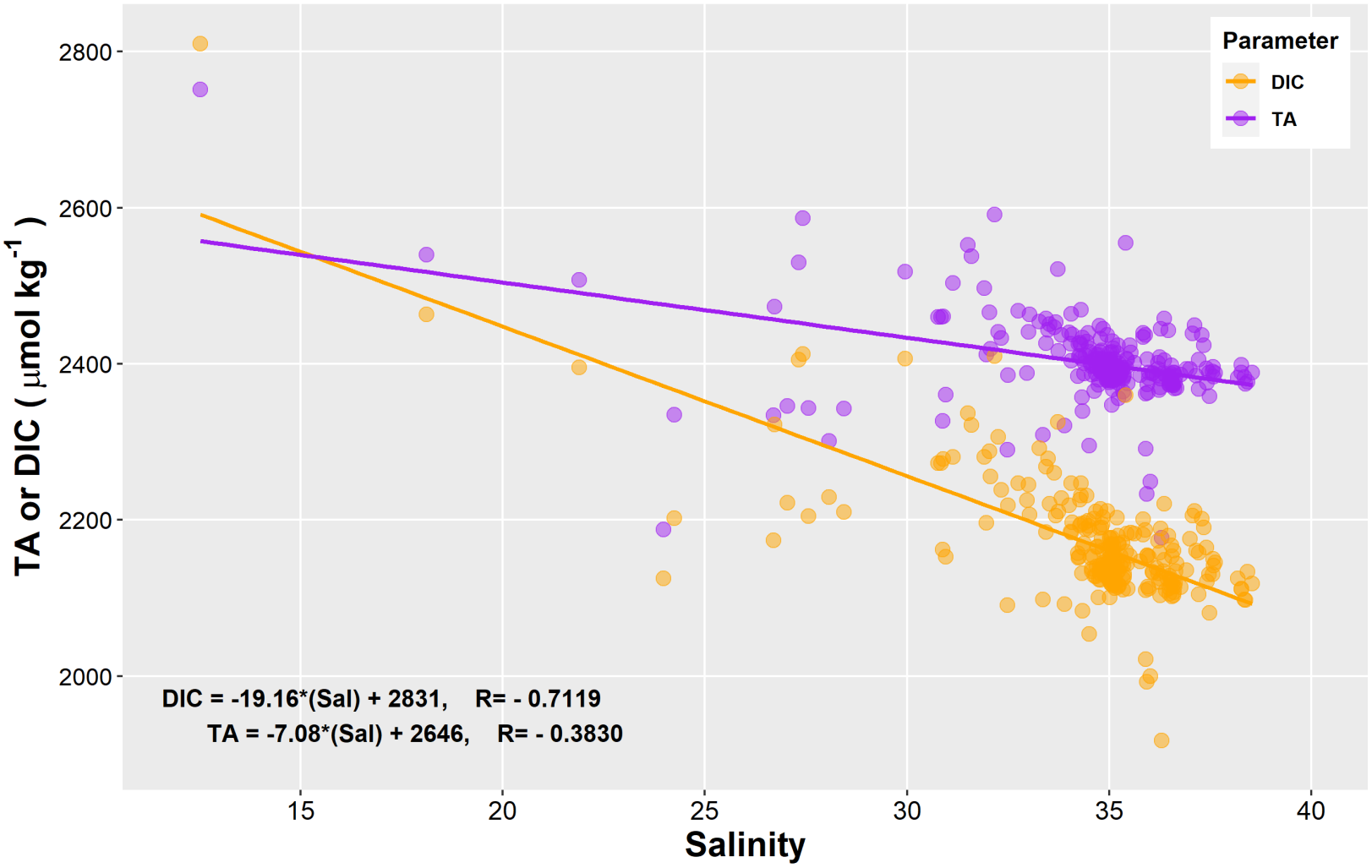


Figure 6. Depicts the relationships between TA (purple) and DIC (orange) versus salinity across the sampled region. Equations for the respective linear relationships are displayed in the lower left. The Y-intercept from these plots predicts the zero salinity TA and DIC endmember.

Table 2. Lists the zero salinity endmembers predicted by each inlet's respective TA versus salinity, DIC versus salinity, and TA:DIC versus salinity relationships.

| | Government Cut (GOC) | | Bakers Haulover (BAK) | | Port Everglades (PEV) | | Hillsboro (HIL) | | Boca Raton (BOC) | | Boynton (BOY) | Lake Worth (ILW) | Jupiter (JUP) | Saint Lucie (STL) | Regional (All Data) | |
|---|---|---|---|---|---|---|---|---|---|---|---|---|---|---|---|---|
| | Inlet | Outfall | Inlet | Outfall | Inlet | Outfall | Inlet | Outfall | Inlet | Outfall | Inlet | Inlet | Inlet | Inlet | Inlet | Outfall |
| **Total Alkalinity ( µmol $kg^{-1}$)** | 3273 | 2633 | 2551 | 2600 | 3105 | 2669 | 3126 | 2512 | 2929 | 2525 | 2358 | 2675 | 2139 | 2016 | 2646 | 2572 |
| **Dissolved Inorganic Carbon ( µmol $kg^{-1}$)** | 3288 | 2888 | 2579 | 2747 | 3139 | 3689 | 3251 | 2598 | 3155 | 2545 | 2662 | 2780 | 2549 | 2192 | 2832 | 2988 |
| **TA:DIC** | 0.9400 | 0.8511 | 0.9642 | 0.8971 | 0.9490 | 0.5029 | 0.8995 | 0.9352 | 0.8951 | 0.9715 | 0.8391 | 0.9381 | 0.7969 | 0.9165 | 0.9022 | 0.7786 |

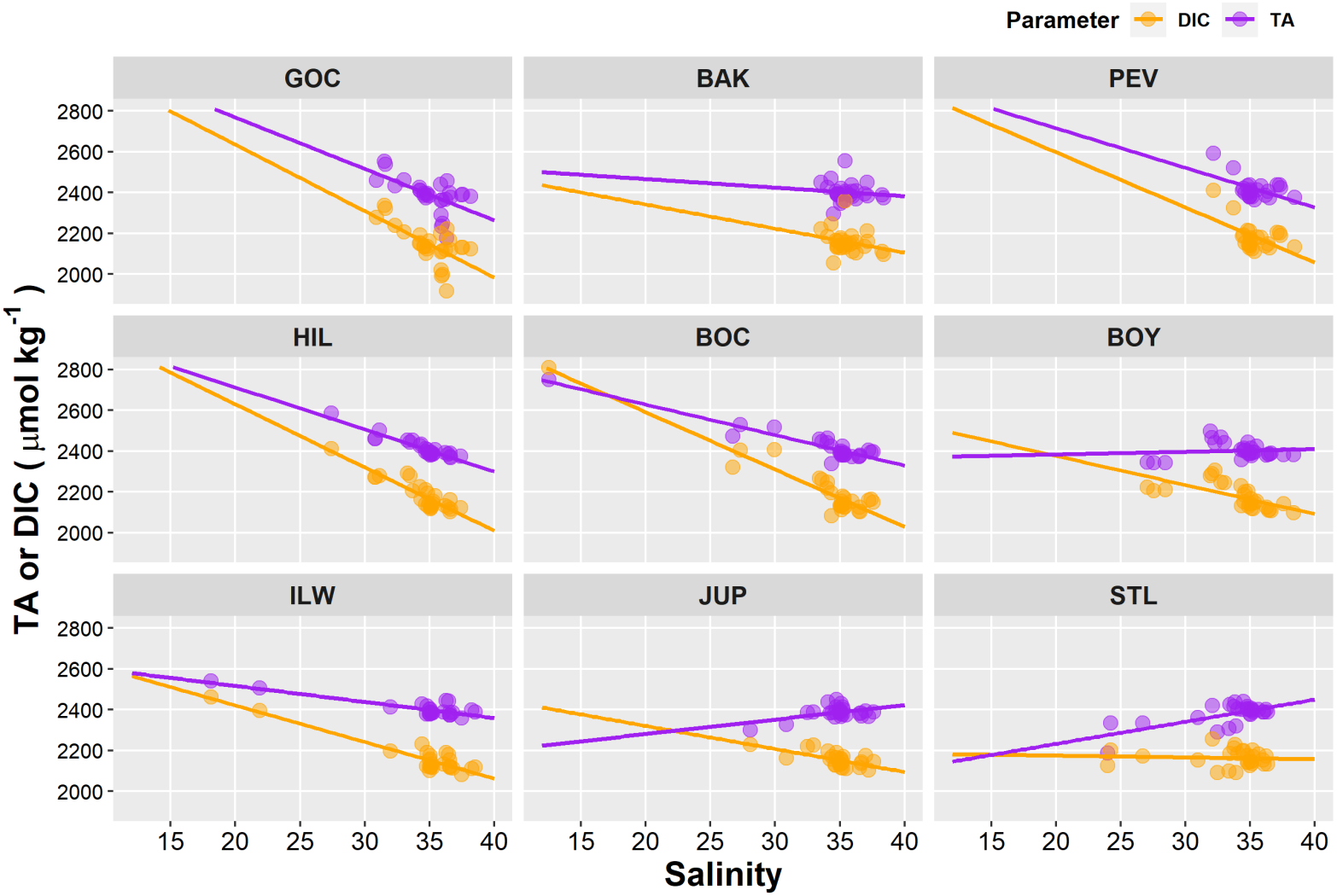


Figure 7. Demonstrates the TA (purple) and DIC (orange) versus salinity relationships of our nine inlet sites. Linear regression lines (least squares) for the corresponding parameter are displayed in their respective color. Inlet locations are ordered in increasing latitude, from left to right, top to bottom, with the farthest south location (GOC) in the top left and most north location (STL) in the bottom right.

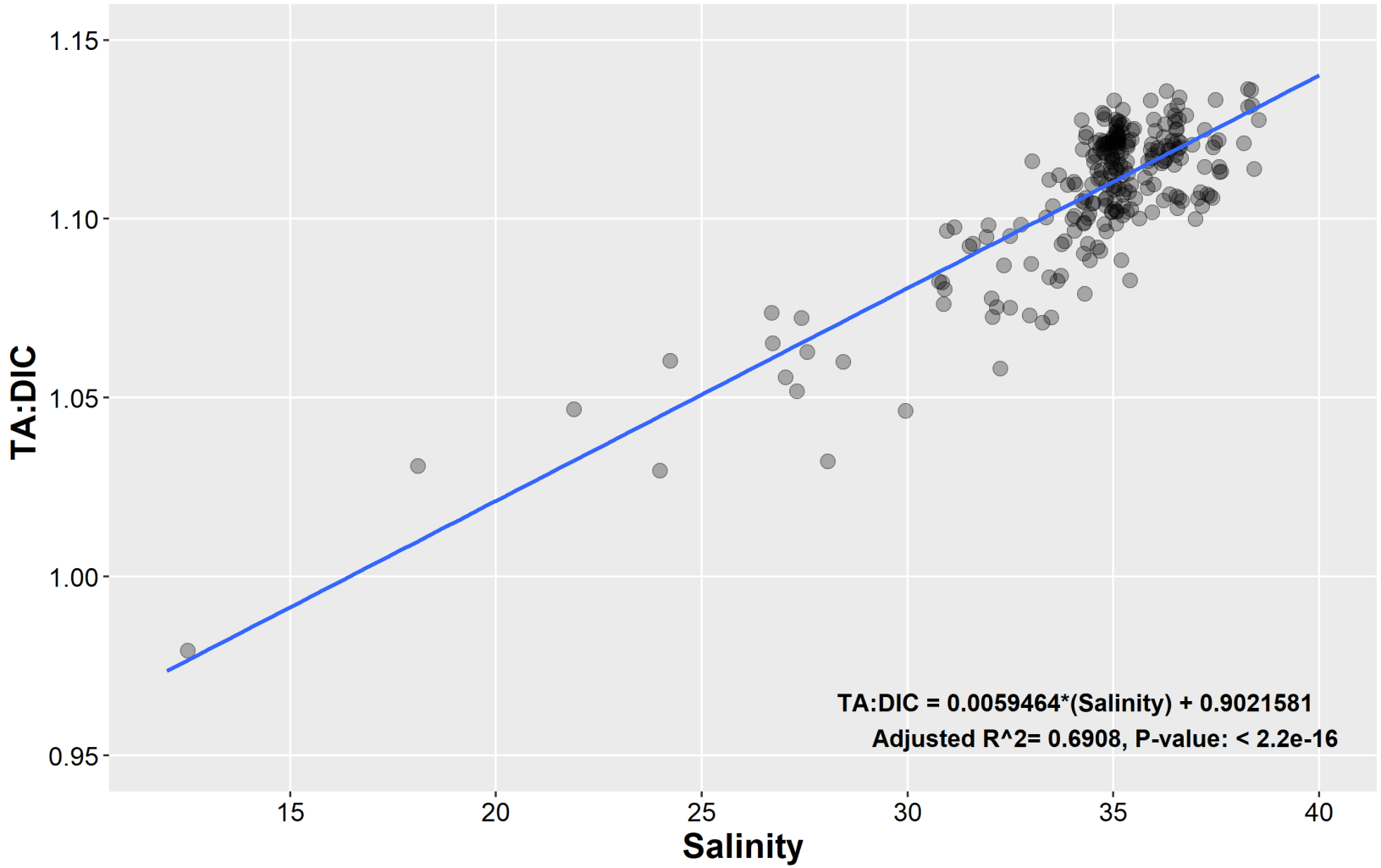


Figure 8. Demonstrates the significant linear relationship between the ratio of TA to DIC (TA:DIC) versus salinity for all inlet data across season and location. Data points are black and the line of best fit (least squares method) is displayed in blue. The equation defining this relationship is displayed in the lower right corner of the plotted area with its corresponding $R^2$ and p-value.

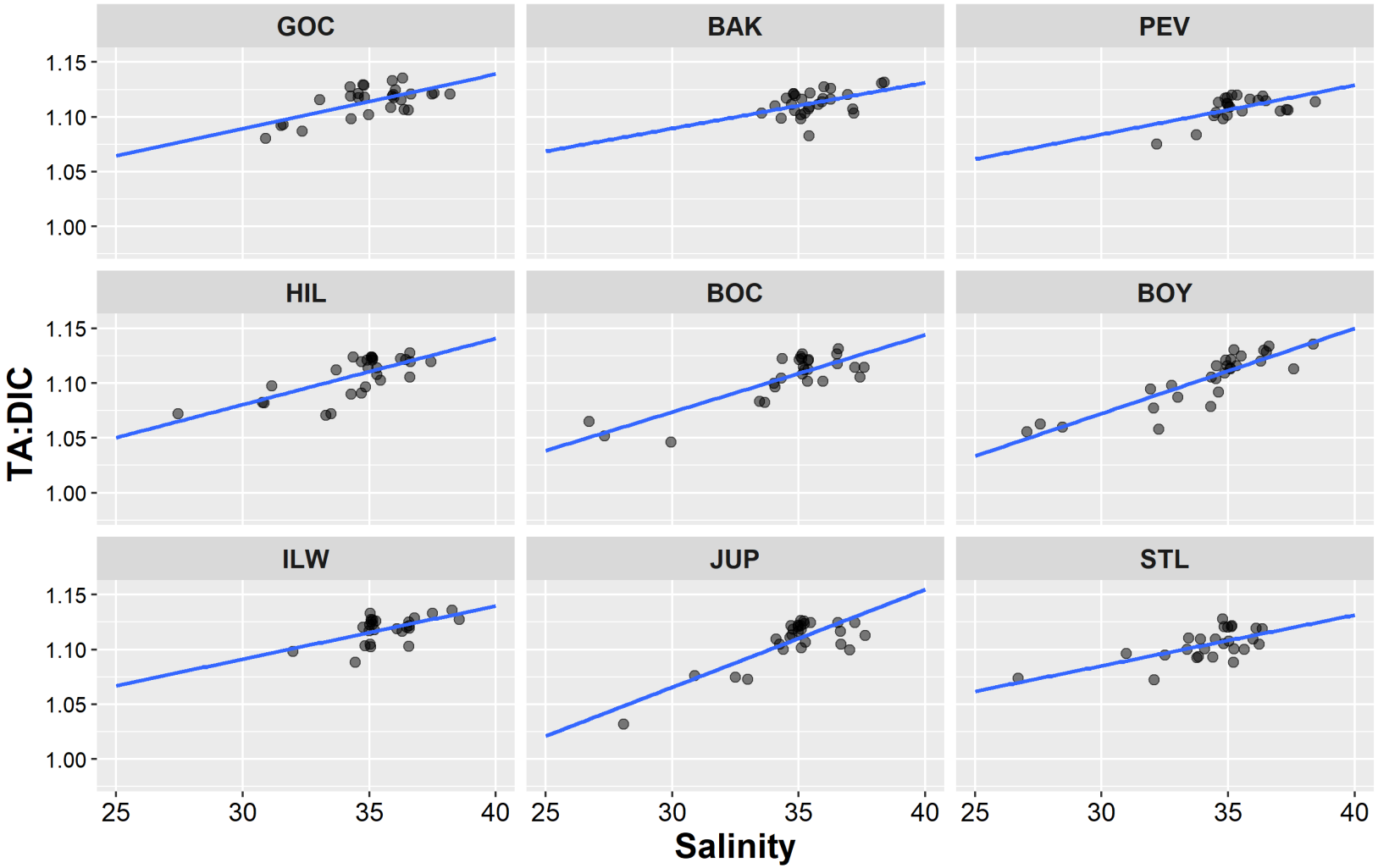


Figure 9. Demonstrates the significant linear relationships between the ratio of TA to DIC (TA:DIC) versus salinity for our 9 inlet sites. Data points are black and the line of best fit (least squares method) is displayed in blue. The salinity scale has been trimmed to a range of 25-40 to emphasize the slopes of each regression.

latitude (Table 2, Figure 10). Latitude had a significant relationship with inlet TA ($p = 0.003$) and DIC ($p = 0.01$), but not TA:DIC endmembers ($p = 0.17$).

### 3.3 Outfall Water Chemistry

Across seasons, DO, temperature, and salinity demonstrated similar means and variance among outfall locations (Table 1). The mean values for pH, $\Omega_{ARAG}$, DIC, and TA were similar across all outfall locations except for site PEV which had greater overall variance and lower mean pH, $\Omega_{ARAG}$, with higher mean DIC. In general, outfall locations demonstrated a small range of observed TA values, with a mean of 2405 µmol $kg^{-1}$ and ranged between 2371 and 2528 µmol $kg^{-1}$. In contrast, the range of DIC values was between 2076 to 2364 µmol $kg^{-1}$, with a mean of 2175 µmol $kg^{-1}$. Across outfall locations, temperature and DO were significantly affected by season, with higher mean temperatures of 28.9 °C and lower mean DO concentrations of 191 µmol $kg^{-1}$ in the wet season. During the dry season, outfalls averaged a temperature of 24.6 °C and a DO concentration of 206 µmol $kg^{-1}$. All other parameters were not significantly affected by season and demonstrated minor differences in mean values.

Across season and sample location, salinity was found to have significant relationships with temperature, DIC, DO, $\Omega_{ARAG}$, and TA:DIC. While the general relationship between TA and salinity was not significant across season and location, these relationships demonstrated across season were generally negative. The slopes of the relationships formed by these regressions were generally more negative in southern locations than the more northerly locations. The relationship between DIC and salinity however, was significantly negatively correlated ($R^2$=0.25). Across seasons, site GOC was the only outfall location to demonstrate a significant relationship between DIC and salinity ($R^2$=0.63). The relationship between DIC and salinity was negative across all locations, generally increasing in slope (less negative) from south to north, aside from PEV. Interestingly, outfall location PEV demonstrated the most negative slope (-41.5 µmol $kg^{-1}$ $S^{-1}$) of all outfall locations, with a value more than double the mean slope of its counterparts, however the fit of this regression is relatively weak ($R^2$=0.38). The relationship between TA:DIC and salinity was significantly positively correlated ($R^2$=0.25) across season and sample location. Across season, all sample locations demonstrated a positive relationship between TA:DIC and salinity, however only locations GOC and BAK demonstrated significant relationships, with moderate $R^2$ values of 0.57 and 0.61 respectively. The small range of salinity

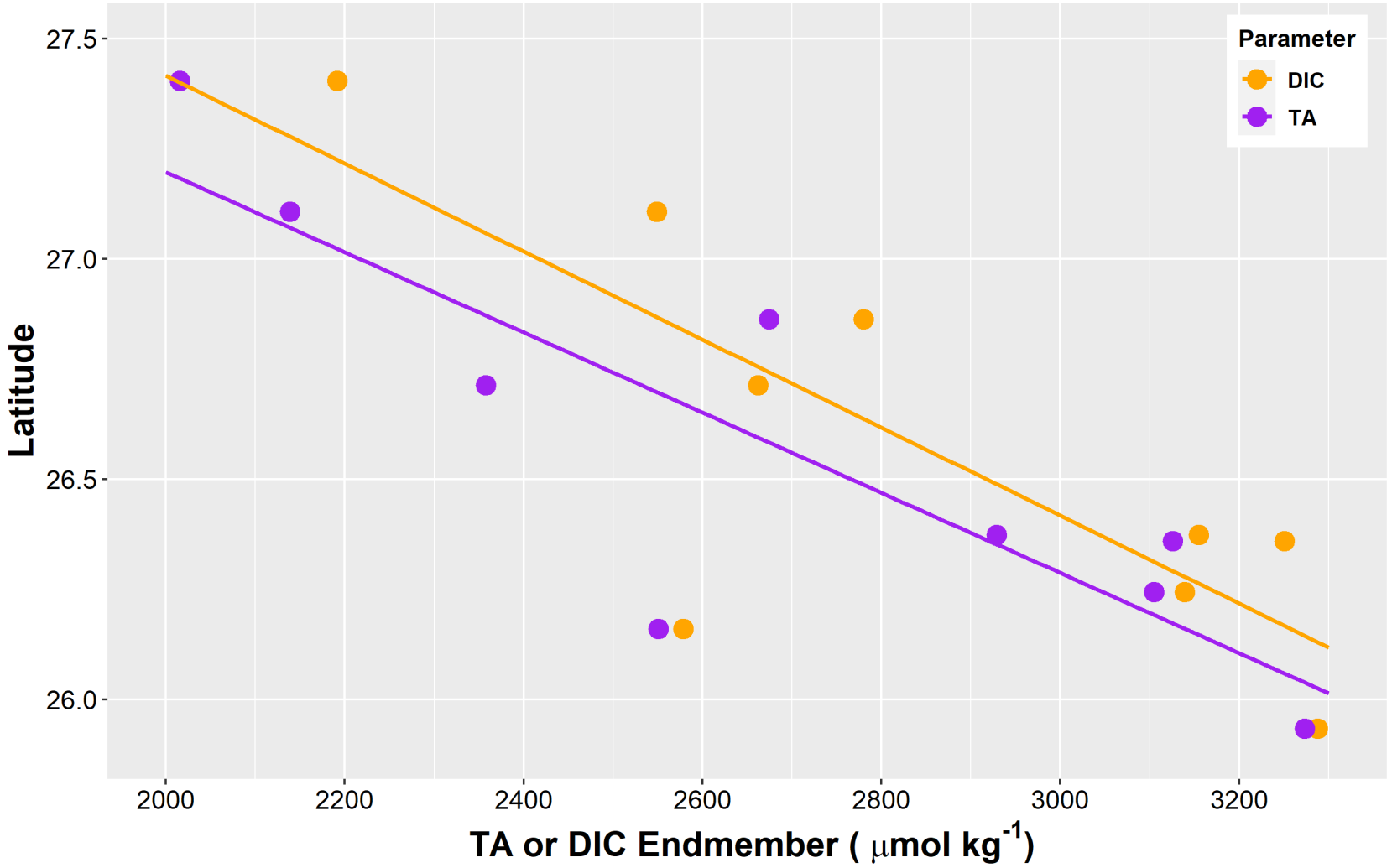


Figure 10. Relationship between latitude versus TA (purple) and DIC (orange) endmembers.

values (33.2-38.3) observed at outfalls makes comparisons between other parameter relationships difficult.

### 3.4 Inlet and Outfall Comparisons

Across seasons, site type (e.g., inlet or outfall) significantly affected salinity values of inlets and outfalls ($p = 0.02$). The means and interquartile ranges (IQR) of the respective site types were similar, though mean inlet salinities and IQR were about 1 PSU lower. The statistical difference observed between inlets and outfalls could be attributed to a greater occurrence of lower salinity values observed at inlet sites (Figures 4 and 5). All other measured or derived parameters investigated during this study were not significantly affected by site type. Across seasons, inlets generally displayed greater amounts of variation and number of outliers within all measured and derived parameters than outfalls.

During the dry season, site type had significant effects on mean DIC, TA, DO, pH, and $\Omega_{ARAG}$. While these differences were significant, the magnitude of differences between inlets and outfalls were generally minor. Dissolved inorganic carbon values were approximately 40 µmol $kg^{-1}$ greater at outfalls than inlets. Outfall TA values occurred over a smaller range than at inlets during the dry season, with an IQR of 12 µmol $kg^{-1}$ and a mean of 2409 µmol $kg^{-1}$, as opposed to the inlet's IQR of 32 µmol $kg^{-1}$ and mean of 2403 µmol $kg^{-1}$. Dissolved oxygen, pH, and $\Omega_{ARAG}$ were generally greater at inlets than outfalls during the dry season. Site type did not have a significant effect on temperature or salinity during the dry season.

During the wet season, site type had a significant effect on salinity ($p = 0.007$). On average, the mean and IQR of inlet salinities were more than 1 unit lower than the respective ranges of outfall salinities. The majority of inlet low salinity outliers were observed during the wet season and could have caused these significant differences (Figures 4 and 5). All other parameters, both measured and derived, were not significantly affected by site type during the wet season and were generally more variable during the wet season than the dry.

## 4. DISCUSSION

Characterization of water chemistry parameters through temporal and spatially organized frameworks allowed us to explore SE Florida's nearshore carbonate chemistry regimes. The observed changes in marine chemistry were primarily influenced by the freshwater effluent being introduced to nearshore ecosystems through SE Florida's nine navigational inlets. Sources of this freshwater include the diverted water flows from Florida's Kissimmee, Okeechobee, Everglades (KOE), and chain-of-lakes basins. While in transit to the ocean, these diverted water flows accumulate various biogeochemical signals whose modifications to carbonate chemistry are the product of biotic and abiotic processes and reflect the environmental conditions of the habitats traversed (Score & Jacoby, 2006). Therefore, effluent discharged through SE Florida's inlets contained a mixture of local, regional, and oceanic biogeochemical signals. Analyzing how environmental parameters change in relation to salinity provides critical information on what biogeochemical interactions could be influencing SE Florida's carbonate chemistry as well as what effects their cumulative signals might have on their nearshore marine environment. We discuss this further in relation to our data in the sections below.

### 4.1 Average Environmental Conditions within Inlets

Across the eight seawater parameters, inlets generally displayed similar mean values between locations. Compared to the open ocean, the mean TA of inlet sites (2401 μmol $kg^{-1}$) was about the same, though inlet DIC concentrations were higher than normal at 2169 μmol $kg^{-1}$ (Table 1). The elevated regional mean DIC concentration likely explains the lower than normal mean pH (7.88) and $\Omega_{ARAG}$ (2.80). Despite similar mean values, some inlets like Boca Raton had a greater number of outliers when compared to other inlets (Figure 3). These observed differences could have been the product of many interacting factors such as inlet design, local biogeochemical interactions, volume of effluent discharge, or limitations imposed by the sampling design. For example, the extreme salinity (12.5), TA (2752 μmol $kg^{-1}$), and DIC (2810 μmol $kg^{-1}$) observed at Boca inlet on 10/25/2020 were caused by a severe rainfall event (Figure 6). Our study design does not account for weather events, and it could be possible that some inlets were sampled more frequently during weather events that could have had a strong influence on inlet seawater chemistry. Future studies could improve upon these results by expanding the list of measured parameters to include nutrients like nitrogen or sulfates in

addition to collecting data within the ICW and primary KOE drainage canals. These modifications could provide higher resolution data for biogeochemistry analysis and enhance the accuracy of predicted freshwater endmembers. The difficulties associated with enhancing temporal or spatial data resolution within this study design could be partially mitigated with remote sensing technologies, though TA and DIC data would still need to be hand collected for laboratory analysis.

### 4.2 Impacts of Salinity on Inlet Seawater Chemistry

Results from the TA and DIC versus salinity relationships support two main conclusions (Figure 6 and 7). First, the freshwater effluent exiting SE Florida's inlets is introducing total alkalinity and dissolved inorganic carbon at elevated levels in relation to the surrounding marine environment. Secondly, the freshwater effluent across this region is introducing DIC in disproportionately greater amounts than TA (Table 2). Support for both of these conclusions can be found in the y-intercept defined by each parameter's linear regression line, as this value is the predicted parameter value or "endmember" for water with a salinity of 0, or freshwater. Based on these relationships, SE Florida's regional freshwater effluent would be expected to have TA and DIC concentrations of 2646 μmol $kg^{-1}$ and 2832 μmol $kg^{-1}$, respectively (Table 2, Figure 6). In contrast, open ocean TA and DIC endmembers estimated from a regionally appropriate dataset (Bermuta Atlantic Time-series Study or BATS, 2019), predict local offshore TA and DIC concentrations of 2401 μmol $kg^{-1}$ and 2077 μmol $kg^{-1}$ for a salinity of 36.6 (Bates & Johnson, 2020). The elevated freshwater TA and DIC concentrations observed in our data are similar to rivers with large drainage basins or high discharge volumes. For instance, the Mississippi-Atchafalaya River system ranked as the world's 3$^{rd}$ largest river in terms of drainage basin area or 7$^{th}$ largest in terms of freshwater discharge volumes (Cai et al., 2008), is estimated to have near zero salinity TA and DIC endmembers of 2920 μmol $kg^{-1}$ and 2870 μmol $kg^{-1}$ respectively (Cai, 2003). The Amazon, the world's largest river in terms of basin area, discharge volume, and total DIC exports predicts zero salinity TA and DIC endmembers of 600 μmol $kg^{-1}$ (Ternon et al., 2000). Riverine TA and DIC concentrations are complex functions of local bedrock and sediment compositions/erosional properties, land use cases across the drainage basin, discharge volumes, seasonal precipitation regimes, and much more (Cai et al., 2008). Therefore, there is large variation in the amount of TA and DIC being exported by rivers. Submarine groundwater discharge (SGD) also has the potential to be a large contributor to the freshwater DIC and TA

endmembers observed in our data. Within coastal ecosystems, SGD can comprise some 6-10% of surface water flows with porewater $HCO_3^-$ concentrations ranging from 95-13000 µmol $L^{-1}$ (Rad et al., 2007). It is likely that biogeochemical modifications of the freshwater as it transits the KOE watershed are leading to this increase in TA and DIC (discussed in more detail below).

The TA and DIC zero salinity endmembers varied across the different inlets (Table 2, Figure 7). Plotting each inlet's freshwater endmembers against latitude reveals a geographical trend in freshwater carbonate chemistry along SE Florida's coastline (Figure 10). Both TA and DIC freshwater endmembers form significant ($p < 0.02$) negative linear relationships with latitude, indicating increased concentrations of both parameters as you move south through the watershed. One hypothesis that could explain these results is that the biogeochemical processes elevating freshwater TA and DIC concentrations are changing with latitude. Also, a longer residence time as water traverses the Everglades from Lake Okeechobee, eventually being discharged along the coast could lead to the accumulation of both TA and DIC (Score & Jacoby, 2006). Freshwater that is being released from inlets at lower latitudes likely traveled a greater distance and remained within SE Florida's canals for longer time periods. The increased residence times of entrained effluents could provide the necessary time for these processes to occur and accumulate various biogeochemical signals. It is impossible to specify exactly what is causing the observed latitudinal trend based on the limitations of this dataset, but the trends are an interesting observation that warrant further investigation.

### 4.3 Implications for Ocean Acidification

To understand how this biogeochemically altered freshwater effluent will affect SE Florida's nearshore ecosystems, we must consider its cumulative effect on carbonate chemistry. Biogeochemical processes that modify TA and DIC act in accordance with their stoichiometric reaction scheme and can occur simultaneously or separately in space and time (Table 3). These modifications to TA and DIC ratios are critically important to nearshore marine ecosystems because the ratio of TA to DIC (TA:DIC) is the primary biogeochemical control of pH within marine environments (Krumins et al., 2013; Wolf-Gladrow et al., 2007). As seen in Figure 11, the data forms a significant ($p < 0.001$) positive linear relationship between TA:DIC and pH, demonstrating that water with lower TA:DIC has reduced pH values. In addition to pH, TA:DIC also affects the buffering capacities of marine systems. Buffering capacity has multiple

definitions, but overall a well buffered aquatic system with high TA:DIC experiences smaller changes to pH per unit changes in DIC (Egleston et al., 2010). Reducing TA:DIC would effectively reduce nearshore buffering capacities and increase the magnitude of pH change caused by the uptake of atmospheric $CO_2$. Lastly, reductions in TA:DIC ratio will also cause aragonite saturation state ($\Omega_{ARAG}$) to decrease. The significant ($p < 0.001$) positive linear relationship between pH and $\Omega_{ARAG}$ (Figure 12) demonstrates that these parameters remain coupled within the SE Florida estuarine system, although this isn't always the case in nearshore

Table 3. Summarizes a few biogeochemical processes that alter TA and DIC concentrations within marine environments. Listed are the stoichiometric equations of the respective processes, in addition to the net TA and DIC changes each process causes. Table adapted from Sippo et al., 2016 and Krumins et al., 2013.

| Reaction | | | Δ DIC | Δ TA |
|---|---|---|---|---|
| Photosynthesis | $106CO_2 + 16NO_3 + H_3PO_4$ | $(CH_2O)_{106}(NH_3)_{16}(H_3PO_4)$ | -1 | 0.2 |
| $CaCO_3$ Dissolution | $CaCO_3$ | $Ca^{2+} + CO_3^{2-}$ | 1 | 2 |
| CaCO3 Precipitation | $Ca^{2+} + CO_3^{2-}$ | $CaCO_3$ | -1 | -2 |
| Sulfate Reduction | $CH_2O + 0.5SO_4^{2-} + 0.5H^+$ | $CO_2 + 0.5HS^- + H_2O$ | 1 | 1 |
| Sulfide Oxidation | $0.5HS^- + O_2$ | $0.5SO_4^{2-} + 0.5H^+$ | 0 | -1 |
| Denitrification | $CH_2O + 0.8NO_3^- + 0.8H^+$ | $CO_2 + 0.4N_2 + 1.4H_2O$ | 1 | 0.8 |
| Nitrification | $0.5NH_4^+ + O_2$ | $0.5NO_3^- + 0.5H_2O + H^+$ | 0 | -1 |
| Iron Reduction | $CH_2O + 4Fe(OH)_3 + 8H^+$ | $CO_2 + 4Fe^{2+} + 11H_2O$ | 1 | 8 |
| Iron Oxidation | $4Fe^{2+} + O_2$ | $4Fe(OH)_3 + 8H^+$ | 0 | -8 |

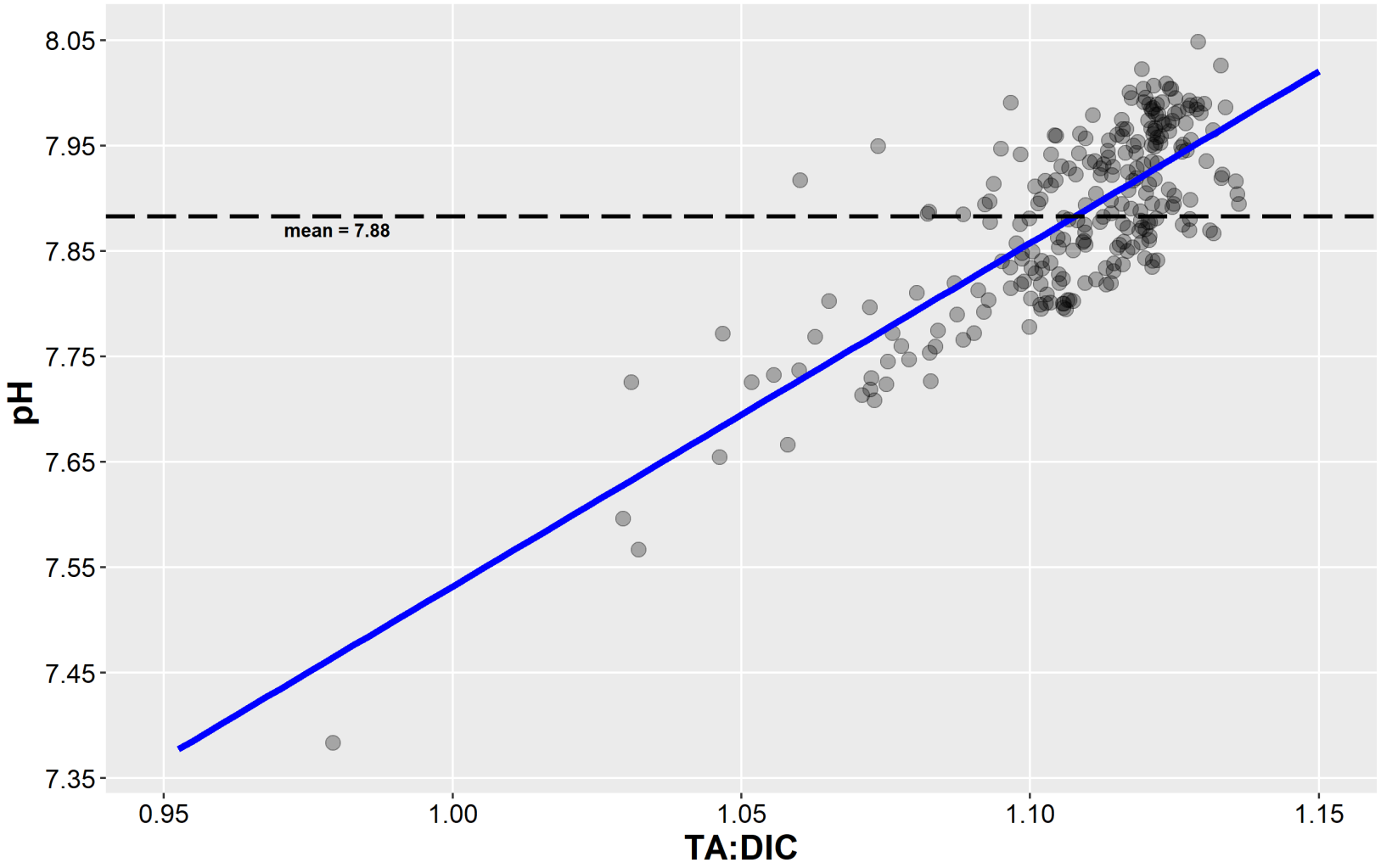


Figure 11. Demonstrates the significant linear relationship between the ratio of TA to DIC (TA:DIC) to pH. Data points are black and the line of best fit (least squares method) is displayed in blue. The mean pH of these data is designated as a black horizontal dashed line, with the mean value displayed below the line

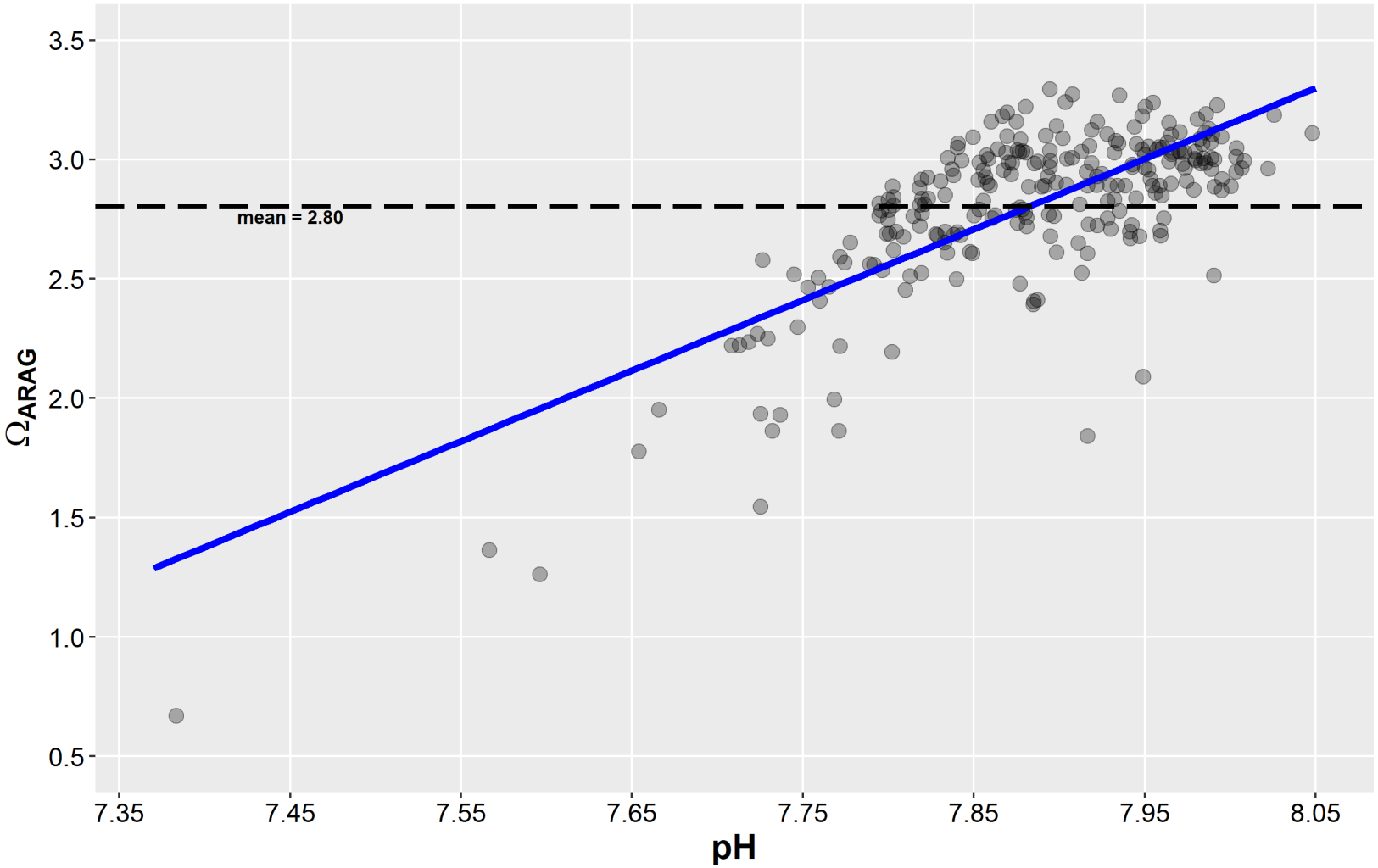


Figure 12. Demonstrates the significant linear relationship between the ratio of pH and Aragonite saturation state ($\Omega_{ARAG}$). Data points are black and the line of best fit (least squares method) is displayed in blue. The mean $\Omega_{ARAG}$ of these data is designated as a black horizontal dashed line, with the mean value displayed below the line

environments (Feely et al., 2018; Fassbender et al., 2016). When TA:DIC data is plotted against to salinity (Figure 8), a significant ($p < 0.001$) positive linear relationship is formed. This relationship clearly demonstrates the control that salinity has on the coastal carbonate system when low TA:DIC freshwater is mixed with saline open ocean water. In total, regional biogeochemical processes and mixing are reducing SE Florida's nearshore pH, $\Omega_{ARAG}$, and buffering capacities, potentially altering local ocean acidification trajectories as seen in other coastal systems (Su et al., 2020; Pacella et al., 2018; Shaw et al., 2012). Further high-resolution monitoring of carbonate chemistry variability within SE Florida coastal systems will be necessary to determine how OA impacts local SE Florida ecosystems.

We can hypothesize which inlet locations are more vulnerable to OA by assessing how their carbonate chemistries change in relation salinity (Figure 9). Each inlet forms significant ($p<0.02$) positive linear relationships between TA:DIC and salinity, providing additional support for our previous conclusion that lower salinity water is introducing DIC in disproportionally greater amounts than TA across this region. Most importantly, the slope defining each linear relationship is indicative of location specific buffering capacities across mixing salinity profiles, with greater slope values indicating lower buffering capacities across the salinity gradient. Based on this, Jupiter inlet has the lowest buffering capacities of SE Florida's inlets, followed closely by inlets BOY, BOC, and HIL. However, this analysis is based on TA:DIC relationships with salinity, which may not tell the full story. A different approach to examine inlet specific buffering capacities is to compare the relationships between TA and DIC (Deffeyes, 1965). Similar to the latitudinal trend observed with salinity, the TA-DIC slope of each inlet shows a relationship with higher slopes in the more southern inlets (Figure 13). Jupiter inlet is the most sensitive to DIC perturbations, owing to its very low TA-DIC slope (0.035), which indicates that net changes to TA and DIC cause large changes in pH across isoclines (Figure 14). On the other hand, Saint Lucie inlet is among the least sensitive locations to DIC acidification events, along with the southern inlets PEV, BAK, and GOC. This indicates that ocean acidification will proceed dynamically along the South Florida coast.

### 4.4 Biogeochemical Processes Impacting Carbonate Chemistry

The TA and DIC relationships we observed at each inlet are the products of both mixing water masses and biogeochemical processes. Active biogeochemical processes can alter TA and

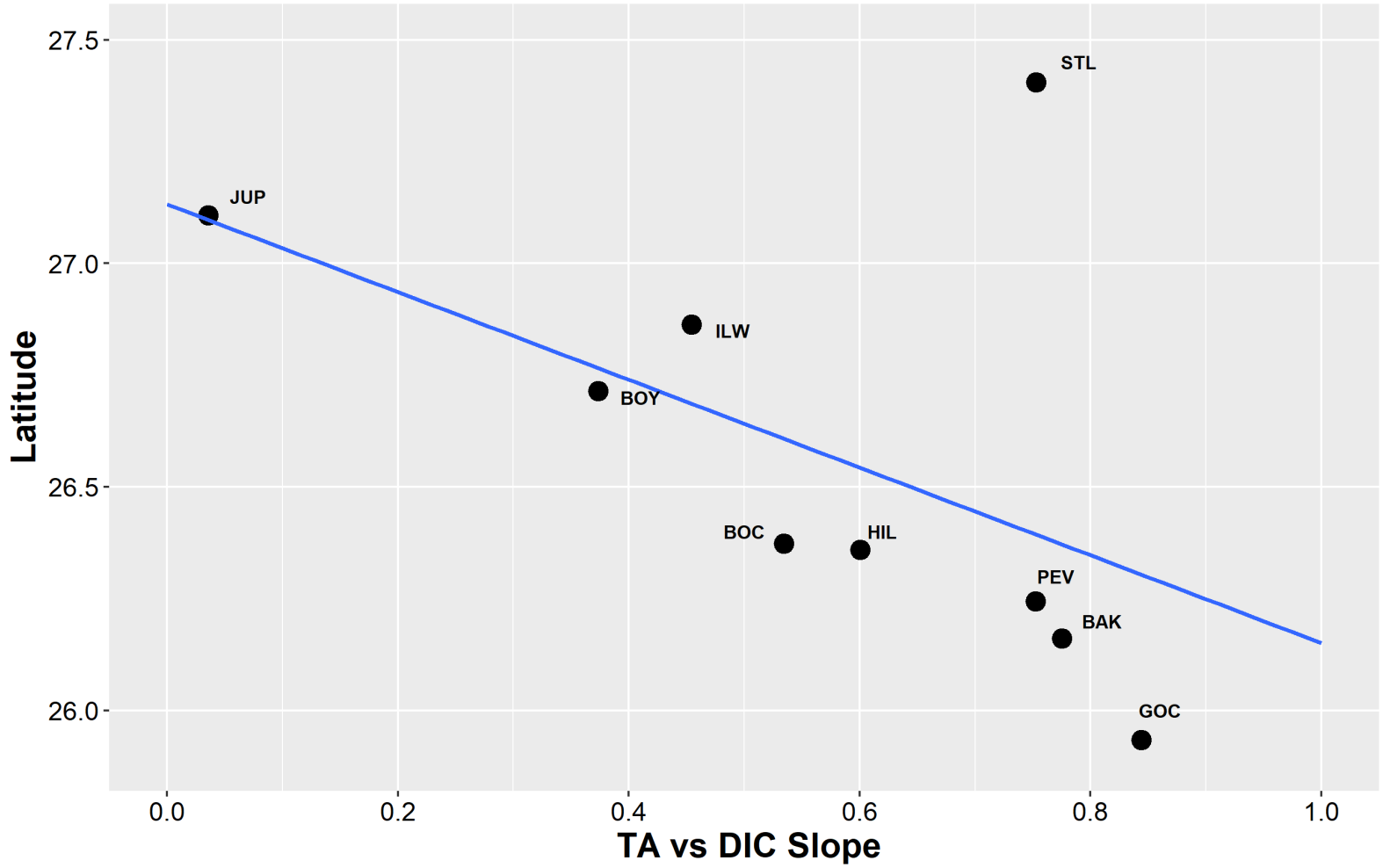


Figure 13. Displays Latitude in relation to each inlet's TA-DIC slope, with a line of best fit (least squares) displayed in blue. Each data point represents an individual inlet location, with that inlet's TA-DIC slope value plotted on the X-axis and the latitude of the corresponding site plotted on the Y-axis. Each data point is accompanied by its respective name abbreviation to simplify identification. Inlets located closer to the Y-axis are more sensitive to DIC.

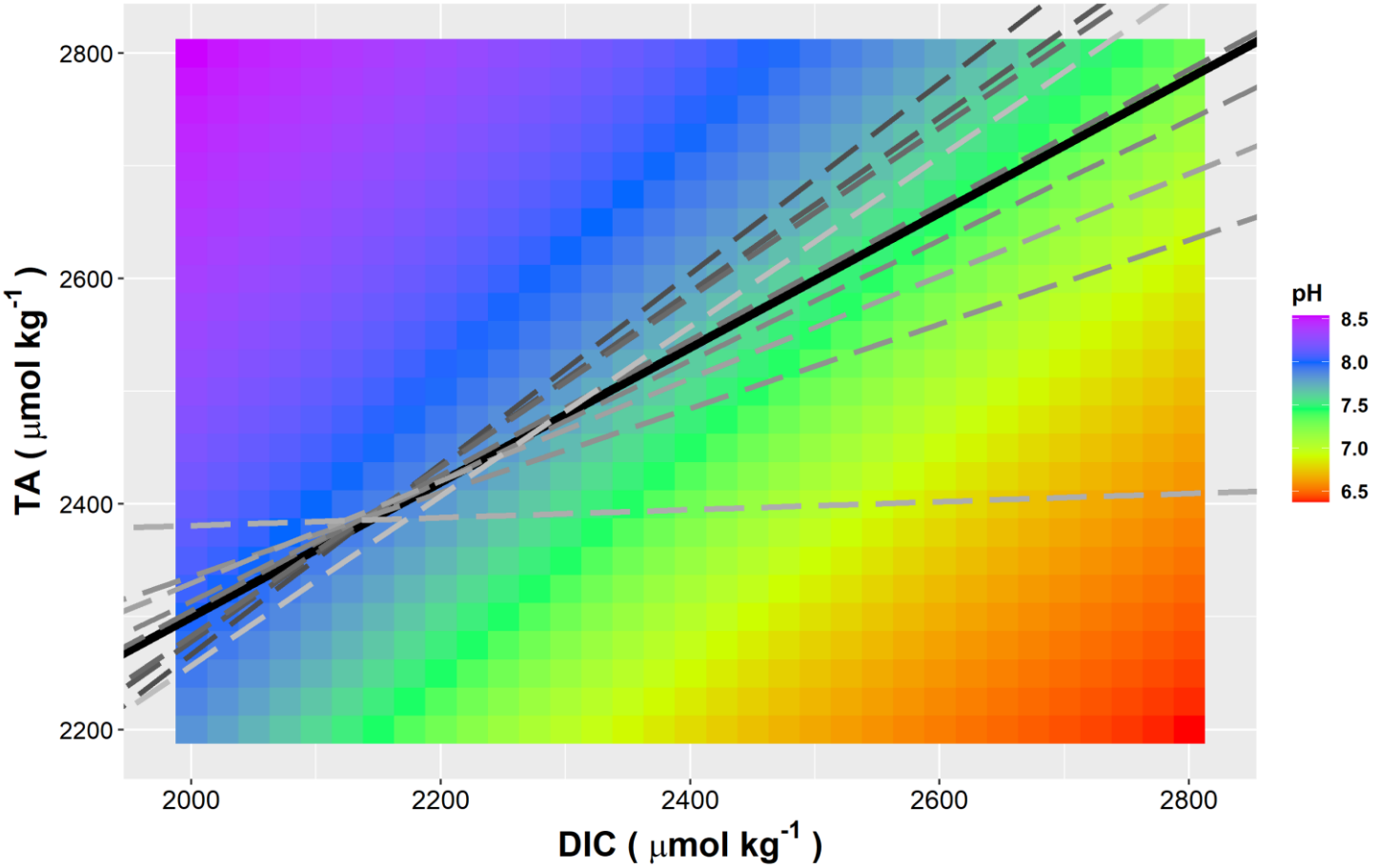


Figure 14. Demonstrates the sensitivity of individual inlets to DIC. The linear regressions defining each inlets relationship between TA and DIC or (TA-DIC) are displayed as dashed lines in greyscale. Inlet regressions are shaded lightest to darkest in increasing latitude, from south to north. Inlet GOC has the lightest shade of grey, while inlet STL has the darkest shade of grey. The regional TA-DIC trend is displayed as a solid black line. The approximate pH values of water samples at any given TA and DIC value are plotted in the background to demonstrate how each inlet's pH will change in response to DIC, with lower slope values crossing pH isoclines at more perpendicular angles.

DIC concentrations within estuarine systems and are reflected in their impacts to carbonate chemistry (Sippo et al., 2016; Krumins et al., 2013). Several common biogeochemical processes impacting nearshore carbonate chemistry are listed in Table 3. Analysis of each inlet's TA versus DIC relationship will allow us to hypothesize which processes have greater influence on the overall TA and DIC relationship, although this is also influenced by water mass mixing. Many of these biogeochemical processes are not mutually exclusive and operate at different reaction rates, therefore the exact combination of processes that are producing the signals we observe in our zero salinity endmembers cannot be identified, though they can be hypothesized. The elevated TA and DIC freshwater endmembers suggest the most influential processes within our study region to be contributors of TA and DIC. The linear relationship defining SE Florida's regional TA and DIC concentrations suggests a slope of 0.60, meaning the processes elevating these parameters would also need to disproportionately increase DIC.

Calcium carbonate dissolution could be producing the strong TA signal we observe, as this process increases TA and DIC at a rate of 2:1 and is ubiquitous across Florida's environments (Middelburg, 2020). Calcium carbonate sediments form the basis of Florida's limestone bedrock and is frequently used as a nutrient supplement for agricultural processes in the form of lime ($CaCO_3$). Aerobic respiration likely serves a large role in the DIC signal we observe as well, which reduces TA and increases DIC at in a 0:1 ratio. These two processes combined equally will produce a TA-DIC slope of 1. Considering the range (0.84-0.04) of inlet specific TA-DIC slopes we observed, it is likely that these two processes alone make up substantial portion of the observed TA and DIC signal for higher slope locations. Inlets like GOC, BAK, PEV, and STL demonstrate the highest TA-DIC slopes with an average of 0.78, meaning processes that increase DIC or reduce TA like nitrification or sulfide/iron oxidation could be occurring to pull these ratios down from 1. Inlets like HIL, BOC, BOY, and ILW displayed TA-DIC slopes ranging from 0.6-0.37 which could be caused by sulfide oxidation/nitrification. If equally weighted (all occur at the same rate), the slope of these combined processes would be reduced to 0.4 and would fit the maximum range of our inlet locations (0.84-0.37), aside from Jupiter inlet. Considering the local environments, it is likely that $CaCO_3$ dissolution, respiration, and sulfate reduction are all playing important roles. No matter what biogeochemical processes are impacting TA and DIC concentrations, systems that have a TA-DIC slopes different from 1 will experience greater changes in pH and omega.

## 5. CONCLUSION

In summary, our data suggests these 9 navigational inlets are introducing biogeochemically influenced freshwater into their surrounding ecosystems that will undoubtedly modify their local marine carbonate chemistry regimes. The freshwater released into these nearshore ecosystems contains disproportionately elevated TA and DIC concentrations that follow an inverse latitudinal trend. Once mixed with locally altered open-ocean saline waters, ecosystems surrounding these inlet locations experience a reduction in buffering capacity, increasing their sensitivity to DIC inputs, which could result in greater variability in carbonate chemistry parameters. These changes to marine chemistry are especially relevant to SE Florida's nearshore reef ecosystems as these habitats are composed of organisms that are critically dependent on their local chemistry regimes. These locally modified chemistries will magnify the effects of OA, likely experiencing more extensive chemical variations over a shorter time frame than those predicted for the open ocean. Our results identify locations like Jupiter inlet whose reduced buffering capacities make them critically sensitive to OA and would encourage monitoring of these areas for OA impacts. Baseline assessments such as this can form the basis for future monitoring efforts to inform land managers on the construction of more accurate ecosystem-based management plans.

## References


Bates, N. R., & Johnson, R. J. (2020). Acceleration of ocean warming, salinification, deoxygenation and acidification in the surface subtropical North Atlantic Ocean. *Communications Earth & Environment*, 1(1), 33. doi:10.1038/s43247-020-00030-5.

Cai, W.-J., Guo, X., Chen, C.-T. A., Dai, M., Zhang, L., Zhai, W., Lohrenz, S. E., Yin, K., Harrison, P. J., & Wang, Y. (2008). A comparative overview of weathering intensity and HCO3− flux in the world's major rivers with emphasis on the Changjiang, Huanghe, Zhujiang (Pearl) and Mississippi Rivers. *Continental Shelf Research*, *28*(12), 1538-1549. https://doi.org/https://doi.org/10.1016/j.csr.2007.10.014

Cai, W. J. (2003). Riverine inorganic carbon flux and rate of biological uptake in the Mississippi River plume. *Geophysical Research Letters*, *30*(2).

Camp, E. F., Smith, D. J., Evenhuis, C., Enochs, I., Manzello, D., Woodcock, S., & Suggett, D. J. (2016). Acclimatization to high-variance habitats does not enhance physiological tolerance of two key Caribbean corals to future temperature and pH. *Proceedings of the Royal Society B: Biological Sciences*, *283*(1831), 20160442.

Challener, R. C., Robbins, L. L., & McClintock, J. B. (2015). Variability of the carbonate chemistry in a shallow, seagrass-dominated ecosystem: implications for ocean acidification experiments. *Marine and Freshwater Research*, *67*(2), 163-172.

Chan, N. C., & Connolly, S. R. (2013). Sensitivity of coral calcification to ocean acidification: a meta-analysis. *Global Change Biology*, *19*(1), 282-290.

Cyronak, T., Takeshita, Y., Courtney, T. A., DeCarlo, E. H., Eyre, B. D., Kline, D. I., Martz, T., Page, H., Price, N. N., & Smith, J. (2020). Diel temperature and pH variability scale with depth across diverse coral reef habitats. *Limnology and Oceanography Letters*, *5*(2), 193-203.

Deffeyes, K. S. (1965). Carbonate equilibria: A graphic and algebraic approach 1. *Limnology and Oceanography*, 10(3), 412-426.

Dickson, A. G., Sabine, C. L., & Christian, J. R. (2007). *Guide to best practices for ocean CO2 measurements*. North Pacific Marine Science Organization.

Doney, S. C., Fabry, V. J., Feely, R. A., & Kleypas, J. A. (2009). Ocean acidification: the other CO2 problem. *Annual review of marine science*, *1*, 169-192.

Duarte, C. M., Hendriks, I. E., Moore, T. S., Olsen, Y. S., Steckbauer, A., Ramajo, L., Carstensen, J., Trotter, J. A., & McCulloch, M. (2013). Is ocean acidification an open-ocean syndrome? Understanding anthropogenic impacts on seawater pH. *Estuaries and Coasts*, *36*(2), 221-236.

Egleston, E. S., Sabine, C. L., & Morel, F. M. (2010). Revelle revisited: Buffer factors that quantify the response of ocean chemistry to changes in DIC and alkalinity. *Global Biogeochemical Cycles*, *24*(1).

Enochs, I. C., Manzello, D. P., Jones, P. R., Stamates, S. J., & Carsey, T. P. (2019). Seasonal carbonate chemistry dynamics on southeast Florida coral reefs: Localized acidification hotspots from navigational inlets. *Frontiers in Marine Science*, *6*, 160.

Eyre, B. D., Andersson, A. J., & Cyronak, T. (2014). Benthic coral reef calcium carbonate dissolution in an acidifying ocean. *Nature Climate Change*, *4*(11), 969-976.

Fassbender, A. J., Sabine, C. L., & Feifel, K. M. (2016). Consideration of coastal carbonate chemistry in understanding biological calcification. *Geophysical Research Letters*, *43*(9), 4467-4476.

Feely, R. A., Okazaki, R. R., Cai, W.-J., Bednaršek, N., Alin, S. R., Byrne, R. H., & Fassbender, A. (2018). The combined effects of acidification and hypoxia on pH and aragonite saturation in the coastal waters of the California current ecosystem and the northern Gulf of Mexico. *Continental Shelf Research*, *152*, 50-60.

Fisher, R., O'Leary, R. A., Low-Choy, S., Mengersen, K., Knowlton, N., Brainard, R. E., & Caley, M. J. (2015). Species richness on coral reefs and the pursuit of convergent global estimates. *Current Biology*, *25*(4), 500-505.

Hunt, C. W., Salisbury, J. E., & Vandemark, D. (2022). Controls on buffering and coastal acidification in a temperate estuary. *Limnology and Oceanography*. doi:https://doi.org/10.1002/lno.12085

IPCC, 2021: *Climate Change 2021: The Physical Science Basis. Contribution of Working Group I to the Sixth Assessment Report of the Intergovernmental Panel on Climate Change* [Masson-Delmotte, V., P. Zhai, A. Pirani, S.L. Connors, C. Péan, S. Berger, N. Caud, Y. Chen, L. Goldfarb, M.I. Gomis, M. Huang, K. Leitzell, E. Lonnoy, J.B.R. Matthews, T.K. Maycock, T. Waterfield, O. Yelekçi, R. Yu, and B. Zhou (eds.)]. Cambridge University Press, Cambridge, United Kingdom and New York, NY, USA, In press, doi:10.1017/9781009157896.

Kapsenberg, L., & Cyronak, T. (2019). Ocean acidification refugia in variable environments. *Global Change Biology*, *25*(10), 3201-3214.

Krimsky, L., Henry, J., & Patterson, J. (2020). Ocean Acidification: pH Variability Across Space and Time: FA227/FA227, 06/2020. *EDIS*, *2020*(5), 4-4.

Kroeker, K. J., Kordas, R. L., Crim, R., Hendriks, I. E., Ramajo, L., Singh, G. S., Duarte, C. M., & Gattuso, J. P. (2013). Impacts of ocean acidification on marine organisms: quantifying sensitivities and interaction with warming. *Global Change Biology*, *19*(6), 1884-1896.

Krumins, V., Gehlen, M., Arndt, S., Van Cappellen, P., & Regnier, P. (2013). Dissolved inorganic carbon and alkalinity fluxes from coastal marine sediments: model estimates for different shelf environments and sensitivity to global change. *Biogeosciences*, *10*(1), 371-398.

Manzello, D. P., Enochs, I. C., Melo, N., Gledhill, D. K., & Johns, E. M. (2012). Ocean acidification refugia of the Florida Reef Tract.

Middelburg, J. J., Soetaert, K., & Hagens, M. (2020). Ocean alkalinity, buffering and biogeochemical processes. *Reviews of Geophysics*, 58(3), e2019RG000681.

Muehllehner, N., Langdon, C., Venti, A., & Kadko, D. (2016). Dynamics of carbonate chemistry, production, and calcification of the Florida Reef Tract (2009–2010): Evidence for seasonal dissolution. *Global Biogeochemical Cycles*, *30*(5), 661-688.

Pacella, S. R., Brown, C. A., Waldbusser, G. G., Labiosa, R. G., & Hales, B. (2018). Seagrass habitat metabolism increases short-term extremes and long-term offset of CO2 under future ocean acidification. *Proceedings of the National Academy of Sciences*, *115*(15), 3870-3875.

Pierrot, D., Lewis, E., & Wallace, D. W. R. (2006). MS Excel program developed for CO2 system calculations. *ORNL/CDIAC-105a. Carbon dioxide information analysis center, oak ridge national laboratory, US Department of Energy, Oak Ridge, Tennessee, 10*.

Price, N. N., Martz, T. R., Brainard, R. E., & Smith, J. E. (2012). Diel variability in seawater pH relates to calcification and benthic community structure on coral reefs.

R Core Team (2021). R: A language and environment for statistical computing. R Foundation for Statistical Computing, Vienna, Austria. URL https://www.R-project.org/.

Rad, S. D., Allègre, C. J., & Louvat, P. (2007). Hidden erosion on volcanic islands. *Earth and Planetary Science Letters*, *262*(1-2), 109-124.

Ries, J. B., Cohen, A. L., & McCorkle, D. C. (2009). Marine calcifiers exhibit mixed responses to CO2-induced ocean acidification. *Geology*, *37*(12), 1131-1134.

Rivest, E. B., Comeau, S., & Cornwall, C. E. (2017). The role of natural variability in shaping the response of coral reef organisms to climate change. *Current Climate Change Reports*, *3*(4), 271-281.

Score, A., & Jacoby, C. (2006). Historical and planned changes in the south Florida ecosystem. *EDIS*, *2006*(33).

Shaw, E. C., McNeil, B. I., & Tilbrook, B. (2012). Impacts of ocean acidification in naturally variable coral reef flat ecosystems. *Journal of Geophysical Research: Oceans*, *117*(C3).

Shaw, E. C., McNeil, B. I., Tilbrook, B., Matear, R., & Bates, M. L. (2013). Anthropogenic changes to seawater buffer capacity combined with natural reef metabolism induce extreme future coral reef CO 2 conditions. *Global Change Biology*, *19*(5), 1632-1641.

Sippo, J. Z., Maher, D. T., Tait, D. R., Holloway, C., & Santos, I. R. (2016). Are mangroves drivers or buffers of coastal acidification? Insights from alkalinity and dissolved inorganic carbon export estimates across a latitudinal transect. *Global Biogeochemical Cycles*, *30*(5), 753-766.

Spalding, M., Burke, L., Wood, S. A., Ashpole, J., Hutchison, J., & Zu Ermgassen, P. (2017). Mapping the global value and distribution of coral reef tourism. *Marine Policy*, *82*, 104-113.

Su, J., Cai, W.-J., Brodeur, J., Chen, B., Hussain, N., Yao, Y., Ni, C., Testa, J. M., Li, M., & Xie, X. (2020). Chesapeake Bay acidification buffered by spatially decoupled carbonate mineral cycling. *Nature Geoscience*, *13*(6), 441-447.

Sunda, W. G., & Cai, W.-J. (2012). Eutrophication induced CO2-acidification of subsurface coastal waters: interactive effects of temperature, salinity, and atmospheric p CO2. *Environmental science & technology*, *46*(19), 10651-10659.

Ternon, J.-F., Oudot, C., Dessier, A., & Diverres, D. (2000). A seasonal tropical sink for atmospheric CO2 in the Atlantic ocean: the role of the Amazon River discharge. *Marine Chemistry*, *68*(3), 183-201.

U.S. Census Bureau (2020). *Florida: 2020 Census*. Retrieved from: https://www.census.gov/library/stories/state-by-state/florida-population-change-between-census-decade.html.

Waldbusser, G. G., & Salisbury, J. E. (2014). Ocean acidification in the coastal zone from an organism's perspective: multiple system parameters, frequency domains, and habitats. *Annual review of marine science*, *6*, 221-247.

Whitall, D. R., Bricker, S. B., Cox, D., Baez, J., Stamates, J., Gregg, K. L., & Pagan, F. E. (2019). Southeast Florida Reef Tract Water Quality Assessment.

Wilson, S. K., Robinson, J. P., Chong-Seng, K., Robinson, J., & Graham, N. A. (2019). Boom and bust of keystone structure on coral reefs. *Coral Reefs*, *38*(4), 625-635.

Wolf-Gladrow, D. A., Zeebe, R. E., Klaas, C., Körtzinger, A., & Dickson, A. G. (2007). Total alkalinity: The explicit conservative expression and its application to biogeochemical processes. *Marine Chemistry*, *106*(1-2), 287-300.